

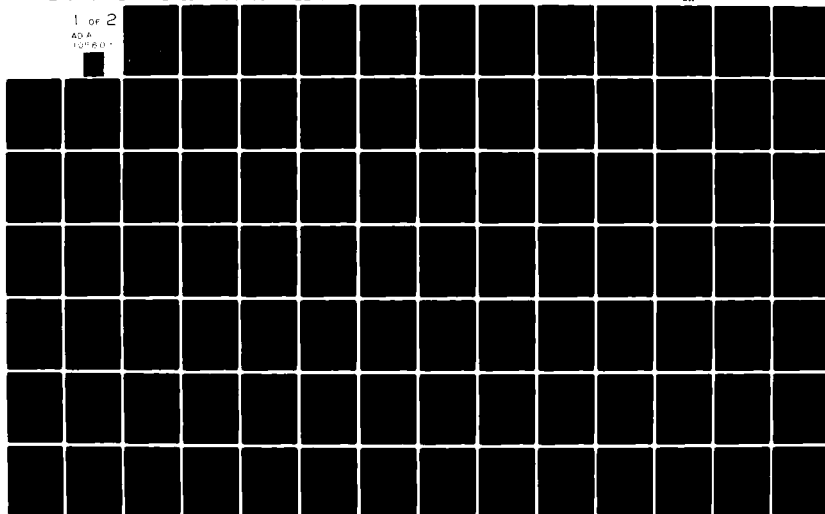
AD-A105 607

FOREIGN TECHNOLOGY DIV WRIGHT-PATTERSON AFB OH  
AIR BREATHING PROPULSION RESEARCH (SELECTED ARTICLES), (U)  
SEP 81 R TSAY, T HSU  
FTD-ID(RS)T-0354-81

F/G 20/4

UNCLASSIFIED

1 of 2  
AD A  
105607



① ②

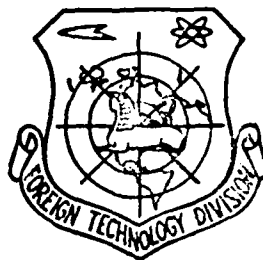
FTD-ID(RS)T-0354-31

AD A105607

# FOREIGN TECHNOLOGY DIVISION



AIR BREATHING PROPULSION RESEARCH  
(Selected Articles)



DTIC  
OCT 7 1981  
A

DTIC FILE COPY

Approved for public release;  
distribution unlimited.

81 10 7 171

# EDITED TRANSLATION

12/107

14 FTD-ID(RS)T-0354-81 11 15 Sep 81  
MICROFICHE NR: FTD-81-C-000843

## AIR BREATHING PROPULSION RESEARCH (Selected Articles)

English pages: 106  
Source: Attachments 1-3 to IR 17510015-80 (China)  
pp 13-49, 1-17, plus 39 unclassified  
pages

Country of origin: China  
Translated by: SCITRAN  
F33657-78-D-0619  
Requester: DIA  
Approved for public release; distribution  
unlimited.

10/1/81  
1/1/81

A

THIS TRANSLATION IS A RENDITION OF THE ORIGINAL FOREIGN TEXT WITHOUT ANY ANALYTICAL OR EDITORIAL COMMENT. STATEMENTS OR THEORIES ADVOCATED OR IMPLIED ARE THOSE OF THE SOURCE AND DO NOT NECESSARILY REFLECT THE POSITION OR OPINION OF THE FOREIGN TECHNOLOGY DIVISION.

PREPARED BY:  
TRANSLATION DIVISION  
FOREIGN TECHNOLOGY DIVISION  
WP-AFB, OHIO.

FTD-ID(RS)T-0354-81

Date 15 Sep 1981

14/1

11/1

## TABLE OF CONTENTS

The Analytical Solution of Mean Stream Line Method for Two-Dimensional Cascades - Some Developments of the Mean Stream Line Method, by Tsay Ruey-shen.....	1
Calculation of Transonic Flow in Planar Cascades - Some Development of Mean Stream Line Method, by Tsay Ruey-shen....	60
Theory of Three-Dimensional Flow in Transonic Turbine Machinery With Shock Wave Interruptions, by Hsu Tsen-chung...	88

THE ANALYTICAL SOLUTION OF MEAN STREAM LINE METHOD  
FOR TWO-DIMENSIONAL CASCADES -  
SOME DEVELOPMENTS OF THE MEAN STREAM LINE METHOD I\*

Tsay Ruey-shen

(Tsing Hua University)

Abstract

This paper presents an improvement for the mean-stream line method - using the analytical solution. This method can drastically speed up the calculation and increase the accuracy of the calculation. In this paper it presents simple equations and tables of functions for convenience of calculation as well as examples of such calculation. In order to convenience the designing, this paper also analyzes preliminarily as to how the design parameters should be chosen in order to obtain the desired turbine blade shape. Using these methods and related information, it can be done in one day to complete the design of a good turbine cascade circulated by compressible flow (if only calculation of incompressible flow is necessary, the speed of computation can still be rised several time). This paper finally also gives a comparison between its results and the experimental data and presents several possible directions under which the mean-stream line method can still be further developed.

SYMBOLS

- A - trigonometric function of  $\beta$
- a - width of the exit in the throat region in the duct between blades

\*This paper has been presented in the First National Meeting of Engineering Thermal Physics in August, 1965.

- B - trigonometric function of  $\beta$ , or the width of the blade in the Z direction
- b - arc length of the blade
- C - trigonometric function of  $\beta$
- $c_p$  - isobaric specific heat of the gas
- D - diameter of the inner circle of the duct between blades
- G - trigonometric function of  $\beta$
- H - trigonometric function of  $\beta$
- i - enthalpy of the gas
- l - blade surface or the arc length of the blade surface
- M - Mach number of the gas flow
- n - the distance in z-direction of the front fringe of the blade at the point where the thickness in the y-direction is the maximum
- P - trigonometric function of  $\beta$
- p - pressure of the gas
- q - an arbitrary physical quantity
- R - gas constant
- r - radius
- T - trigonometric function of  $\beta$
- t - cascade distance of blade cascade
- W - gas flow velocity
- y - coordinate direction (direction of the forehead line of the cascade)
- z - coordinate direction (axial direction of the turbine machinery)
- $\Delta y$  - the absolute value of the distance in the y direction between the mean-stream line and the surface of the blade
- $\beta$  - an angle (starting from the z-coordinate and giving counter clockwise)
- $\delta$  - the thickness of the blade in the y-direction at any point
- $\gamma$  - ratio of specific heats of gas
- $\eta$  - a constant
- $\lambda$  - a constant; or the gas flow velocity divided by the critical velocity, i.e. velocity coefficient
- $\theta$  - a constant

- $\rho$  - the density of gas
- $\omega$  - a function

#### SUPERSCRIPTS

- \* - relative value (divided by the inlet parameter)
- ' - derivative with respect to  $z$
- . - parameter at the rear forehead line of the cascade

#### SUBSCRIPTS

- $o$  - stagnation value
- 1,2,  
3...n - different functions or constants
- B - incompressible
- e - far away downstream of the cascade
- i - far away upstream of the cascade
- m - values on the mean-stream line or values on any selected stream line
- max - maximum value
- p - inner arc of the blade
- s - back arc of the blade
- y - y-direction component
- z - z-direction component
- 60% - values on the stream line which has a 60% flow of that at the back arc.

#### I. Mean-Stream Line Method

The condition of the gas flow circulation through the planar cascade has an extremely large effect on the characteristics of the turbine machinery. Therefore the calculation of the condition of gas flow circulation for a given planar cascade (Forward Problem) and the designing of a planar cascade which has good aerodynamic properties and satisfies certain actual requirements (reverse problem) are both important

subjects to study for people working in the turbine machinery. Up to date, there has been a lot of work done in this area. There are various methods available. Among them there are methods which are based on relatively rigorous theoretical basis such as the conformal transformation method and so on. However, the actual calculation load is relatively large. In addition, it is very difficult to extend to compressible flow and flow on an arbitrarily revolving surface. Pure numerical solution has been used to consider the compressibility of gases but the computational load is too large and it casually requires an electronic computer to carry out the computation. Therefore, on the other hand, some relatively simple approximation methods emerged. For example, the mean-stream line method<sup>[1]</sup> proposed by Professor Wu Ching-hua is one of the effective methods to calculate planar cascades. It has a relatively sophisticated theoretical basis to easily consider the compressibilities of gases. Its computational load is not large and results with sufficient accuracy can be obtained rapidly. In addition, the thickness distribution required in the design work can be easily found in order to assure the strength, rigidity, and cooling requirements. Besides, it can be extended to the more generalized conditions of flow on an arbitrary revolving surface. Therefore, it has already become a generally used computational method worldwide.

The essence of the mean stream line method is as follows: If the shape of a stream line inside the duct of the cascade is known (such as the mean stream line  $y_m = y(z)$  which equally divides the flow on the duct) and the variation pattern of any gas flow parameter on it [such as  $(\rho u)_m = \omega(z)$ ] (refer to Figure 1), then it is possible to use the steady, isentropic, continuous, non-rotational, and ideal gas conditions in aerodynamics to derive the partial derivatives of various orders of the gas parameters on that stream line with respect to the



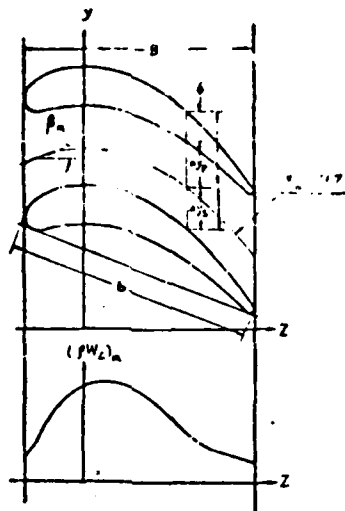


Figure 1. Design Variables in the Mean Stream Line Method

y direction. The actually applicable equations are as follows<sup>[1]</sup>:

$$\rho^* = \frac{\rho}{\rho_i} = \frac{\rho_{0i}}{\rho_i} \left( 1 - \frac{W^2}{2c_0^2} \right)^{1/\gamma-1} \quad (1)$$

$$W_y = W' \sin \beta \quad (2)$$

$$W_z = W' \cos \beta \quad (3)$$

$$\left( \frac{\partial W_y}{\partial y} \right)_m = \left[ \frac{dW_y}{dz} \tan \beta - \frac{1}{\rho} \frac{d(\rho W_z)}{dz} \right]_m \cos^2 \beta_m \quad (4)$$

$$\left( \frac{\partial W_z}{\partial y} \right)_m = \left[ \frac{dW_z}{dz} + \frac{1}{\rho} \frac{d(\rho W_y)}{dz} \tan \beta \right]_m \cos^2 \beta_m \quad (5)$$

$$\left( \frac{1}{\rho} \frac{\partial \rho}{\partial y} \right)_m = - \frac{1}{(\gamma-1)(c_0^2 - W_m^2/2)} \left( W_y \frac{\partial W_y}{\partial y} + W_z \frac{\partial W_z}{\partial y} \right)_m \quad (6)$$

$$\left( \frac{\partial^2 W_y}{\partial y^2} \right)_m = \left[ \frac{2}{\rho^2} \frac{\partial \rho}{\partial y} \frac{d(\rho W_z)}{dz} - \frac{1}{\rho} \frac{d}{dz} \left( \rho \frac{\partial W_z}{\partial y} + W_z \frac{\partial \rho}{\partial y} \right) + \tan \beta \frac{d}{dz} \left( \frac{\partial W_y}{\partial y} \right) \right]_m \cos^2 \beta_m \quad (7)$$

$$\left( \frac{\partial^2 W_z}{\partial y^2} \right)_m = \left[ \frac{d}{dz} \left( \frac{\partial W_y}{\partial y} \right) - \frac{\partial^2 W_y}{\partial y^2} \tan \beta \right]_m \quad (7a)$$

$$\left( \frac{1}{\rho} \frac{\partial^2 \rho}{\partial y^2} \right)_m = \frac{2-\gamma}{\rho_m^2} \left( \frac{\partial \rho}{\partial y} \right)_m^2 - \frac{1}{(\gamma-1)(c_0^2 - W_m^2/2)} \left[ W_y \frac{\partial^2 W_y}{\partial y^2} + W_z \frac{\partial^2 W_z}{\partial y^2} + \left( \frac{\partial W_y}{\partial y} \right)^2 + \left( \frac{\partial W_z}{\partial y} \right)^2 \right]_m \quad (8)$$

$$q(y) = q_m + (y - y_m) \left( \frac{\partial q}{\partial y} \right)_m + \frac{(y - y_m)^2}{2!} \left( \frac{\partial^2 q}{\partial y^2} \right)_m + \frac{(y - y_m)^3}{3!} \left( \frac{\partial^3 q}{\partial y^3} \right)_m + \dots \quad (9)$$

The  $q$  in equation (9) can represent any one of the gas flow parameters. In the actual calculations of the turbine cascade, only the first three terms of the Taylor series expansion will provide sufficient accuracy.

In order to solve the "Forward Problem", at the beginning of the calculation it is necessary to estimate  $y_m = y(z)$  and  $(\rho W_z)_m = \omega(z)$ , under the given duct condition.

In Reference [1], it was believed that the center line of the duct and be used as the first approximation of the mean-stream line (the amount of flow equals on both sides of this line) and the variation of the parameter  $\rho W_z$  along the mean stream line is inversely proportional to the y-direction width of the duct (i.e.  $(\rho W_z)_m \approx \frac{1}{1-\delta}$ ). On this basis of these a preliminary calculation can be carried out. As for whether its results are correct, we can integrate from  $z$ 's on the mean stream line along the  $y$  direction on both sides to determine whether the obtained flow agrees with the incoming flow. Reference [1] also gave a modification method when disagreement was found. Later, in Reference [3], it presented a method to more accurately estimate the position of the mean streamline.

For the "Reverse Problem", if  $y_m = y(z)$  and  $(\rho W_z)_m = \omega(z)$  are given, then all the flow parameters in the flow field can of course be obtained. In the meantime, the boundary of the duct (blade) can also be defined based on the concept of equilibrium flow. Naturally, to obtain good cascades,  $y_m = y(z)$  and  $(\rho W_z)_m = \omega(z)$  also must have certain limitations and matching relations. Reference [3] introduced a method using past experience to plot the shape of the blade and to obtain the approximate variation regularity between the mean stream line and the duct width. Afterwards, the preliminary calculation is carried out followed by gradual improvements.

## II. One Way to Increase the Computational Speed and Accuracy

In the method of using existing mean stream line to design cascades (the Reverse Problem), as described above, because usually the mean stream line and the data of one parameter at several points on it are given (in the past  $\rho W_z$ )

was obtained from consideration of the blade thickness), therefore the numerical differentiation method is used to calculate the derivatives  $\frac{d}{dx}$  along the stream line in equations (4) ~ (7a). This part of the calculation is more time consuming and is difficult to obtain very high accuracy. It is also easier to make mistakes. Because of the use of numerical differentiation equations, the error of one mistakenly calculated point will affect the accuracy of the numerical values thereafter. References [1] ~ [3] suggested the plotting of curves in a table after these derivatives are calculated in order to discover mistakes early and to "polish" the data.

The mean stream line method does not require many computational terms which is one of its advantages. But at least 4 times of numerical differentiation must be calculated. If the five point differentiation equation<sup>[1]</sup> is used, then the computation of each point involves 5 multiplications, 1 addition, and 1 division. In addition, in order to obtain a certain significant figures with accuracy, it is necessary to use more significant figures in the beginning of the calculation. This then becomes a barrier which may not necessarily exist against increasing the computational speed. Besides, the polishing in the numerical calculation, although is an effective method, yet it does not absolutely assure the accuracy of the calculation. Therefore, it is natural to have the following thoughts: Is it possible to change the design of the mean stream line method from variation of parameters to the analytical form? This allows the use of the analytical method in the differentiations and the rearrangement afterwards so that the complicated calculations described above can be eliminated. By doing so it is not necessary to gradually carry out calculations of numerical differentiation to reduce the possibility of computational error. It is also not necessary

to publish the computational results and can obtain the derivatives to an arbitrary degree of accuracy desired. For the logical point of view, this method has no difficulty in the "Reverse Problem". As long as we can find the proper mean stream line and the functional relationship between the flow parameter on it and the z-coordinate. These are not difficult to obtain from the existing cascade data and the computational experience acquired later. Of course, if the equations expressed by the analytical form are too complicated then its meaning is no longer significant. But from the following section, it can be seen that, to the contrary, the use of analytical relations can simplify the equation itself which is more advantageous in computation. Let us elaborate this analytical method in the following.

### III. Analytical Solution of the Reverse Problem

#### 1. Incompressible Flow

Let us first take a look at the special solution to the incompressible flow. At this time equations (1), (4), (5), (7), and (7a) become the following, respectively. (The parameters in this section and in Table 2 in the Appendix are with respect to the mean stream line. For convenience, the subscript is omitted with exception of those specified in the equations):

$$\rho_s^* = \left( \frac{\rho}{\rho_i} \right)_s \equiv 1 \quad (10)$$

$$\left( \frac{\partial W_y}{\partial y} \right)_s = \left( \frac{dW_y}{dz} \tan \beta - \frac{dW_z}{dz} \right)_s \cos^2 \beta \quad (11)$$

$$\left( \frac{\partial W_z}{\partial y} \right)_s = \left( \frac{dW_y}{dz} + \frac{dW_z}{dz} \tan \beta \right)_s \cos^2 \beta \quad (12)$$

$$\left( \frac{\partial^2 W_y}{\partial y^2} \right)_s = \left[ \tan \beta \frac{d}{dz} \left( \frac{\partial W_y}{\partial y} \right) - \frac{d}{dz} \left( \frac{\partial W_z}{\partial y} \right) \right]_s \cos^2 \beta \quad (13)$$

$$\left(\frac{\partial^2 W_z}{\partial y^2}\right)_s = \left[ \frac{d}{dz} \left( \frac{\partial W_y}{\partial y} \right) - \frac{\partial^2 W_y}{\partial y^2} \tan \beta \right]_s \quad (14)$$

If we choose the analytical equation of the mean stream line to be  $y = y(z)$ . In addition, we also choose  $W = W(z)$  as the varying parameter of design instead of  $W_s = \omega(z)$ . This is apparently possible in solving the reverse problem and offers convenience in computation. It makes easier to control the surface velocity distribution of the obtained blade shape. Actually after  $W_s = \omega(z)$  and  $y = y(z)$  are given, then in principle it is completely possible to transform into  $W = W(z)$ . Thus using equations (2), (3), and the above four equations as well as  $\tan \beta = y'(z)$ , it is possible to derive the equation of the analytical solution. However, the operation is rather complicated and the resulted equation is more difficult to use. Therefore, it is better to obtain  $\beta = \tan^{-1}[y'(z)] = \beta(z)$  from  $y = y(z)$  as the varying parameter and then differentiate  $W_y$  and  $W_z$  with respect to  $z$  to carry out the derivation operation. It is then possible to get the simple equations of the partial derivatives of  $W_y$  and  $W_z$  in the  $y$  direction.

$$\left(\frac{\partial W_y}{\partial y}\right)_s = B_3 \cdot W \beta' - B_1 \cdot W' \quad (15)$$

$$\left(\frac{\partial^2 W_y}{\partial y^2}\right)_s = A_1 \cdot W \beta'' + B_6 \cdot W \beta'^2 + A_2 \cdot W' \beta' - B_4 \cdot W'' \quad (16)$$

$$\left(\frac{\partial W_z}{\partial y}\right)_s = B_1 \cdot W \beta' + B_2 \cdot W' \quad (17)$$

$$\left(\frac{\partial^2 W_z}{\partial y^2}\right)_s = B_3 \cdot W \beta'^2 + B_4 \cdot W \beta'' + B_5 W' \beta' + B_6 W'' \quad (18)$$

where  $A_1, A_2, B_1 \sim B_6$  are the simple trigonometric functions of  $\beta$ . For example:

$$A_1 = \cos^2 \beta \sin \beta (12 \cos^2 \beta - 5) \quad (19)$$

$$A_2 = -\cos \beta (16 \cos^4 \beta - 14 \cos^2 \beta + 1) \quad (20)$$

$$B_1 = \cos \beta (2 \cos^2 \beta - 1) \quad (21)$$

$$B_3 = 2 \cos^2 \beta \sin \beta \quad (22)$$

The remaining equations of B can be found in Table 3 in the Appendix.

But in the actual application, it is more convenient to calculate after the values of the partial derivatives of  $W_2$  and  $W$  are obtained. It is because that the former can be used to determine the boundaries of the duct and the latter can be used to directly obtain the velocity distribution with combining the two velocity components to get the velocity. The partial derivative value of  $W$  can be obtained as follows:

Since

$$W^2 = W_1^2 + W_2^2$$

Let us carry out first order and second order partial differentiations on both sides of the above equation. After rearrangement and simplification we get

$$\frac{\partial W}{\partial y} = \frac{\partial W_1}{\partial y} \sin \beta + \frac{\partial W_2}{\partial y} \cos \beta \quad (23)$$

$$\frac{\partial^2 W}{\partial y^2} = \frac{\partial^2 W_1}{\partial y^2} \sin \beta + \frac{\partial^2 W_2}{\partial y^2} \cos \beta + \frac{1}{W} \left[ \left( \frac{\partial W_1}{\partial y} \right)^2 + \left( \frac{\partial W_2}{\partial y} \right)^2 - \left( \frac{\partial W}{\partial y} \right)^2 \right] \quad (24)$$

then substituting equations (15) ~ (18) into the two above equations, we get

$$\left( \frac{\partial W}{\partial y} \right)_s = B_7 \cdot W \beta' + B_8 W' \quad (25)$$

$$\left( \frac{\partial^2 W}{\partial y^2} \right)_s = B_9 \cdot W \beta'^2 + 2B_{10} \cdot W \beta'' + B_{11} \cdot W' \beta' + B_{12} W'' + B_{13} \cdot \frac{W'^2}{W} \quad (26)$$

where  $B_7 \sim B_{13}$  are all simple trigonometric functions of  $\beta$ .

The actual equations can be found in Table 3 in the Appendix.

From these it is found that for incompressible flow the first order and second order partial derivatives in the y direction on the mean stream line are simple linear function of the combination of products of W,  $\beta$  and their partial derivatives with respect to z. Because the coefficients in front of each term are all known simple trigonometric functions of  $\beta$ , table (see Table 3 in the Appendix) can be prepared in advance for future use. After doing so it is very quick to calculate the partial derivatives in the y-directions on the mean stream line. For incompressible flow, after the familiarization of the process, it takes about or less than two hours to calculate over ten points of a duct.

In the next step of determining the position of the boundary of the duct, it is possible to use the partial derivative values everywhere on the mean stream line and the continuity equation to derive a third order algebraic equation to replace the numerical integration method used in the past.

Since

$$\frac{1}{2}W_{z,t} = \int_0^{\Delta y_p} W_z d(\Delta y)^*$$

and

$$W_z = W_{z,m} + \left(\frac{\partial W_z}{\partial y}\right)_m \Delta y_p + \frac{1}{2} \left(\frac{\partial^2 W_z}{\partial y^2}\right)_m \Delta y_p^2$$

We can get

$$W_{z,m} \Delta y_p + \frac{1}{2} \left(\frac{\partial W_z}{\partial y}\right)_m \Delta y_p^2 + \frac{1}{6} \left(\frac{\partial^2 W_z}{\partial y^2}\right)_m \Delta y_p^3 = \frac{1}{2} W_{z,t} \quad (27)$$

Similarly

$$W_{z,m} \Delta y_i - \frac{1}{2} \left(\frac{\partial W_z}{\partial y}\right)_m \Delta y_i^2 + \frac{1}{6} \left(\frac{\partial^2 W_z}{\partial y^2}\right)_m \Delta y_i^3 = \frac{1}{2} W_{z,t} \quad (28)$$

\*The  $W_z$  in these two equations represents the axial velocity component in the direction of gas flow at any point in the duct. It is different from the axial velocity component on the mean stream line in other places of this section.



where absolute values are used for  $\Delta x$ , and  $\frac{1}{2}W_{x,r}$ .

Of course, it is not a simple matter to rigorously solve the third order algebraic equation (although it can be obtained completely).<sup>\*\*</sup> But its approximate solution with a certain accuracy can be easily obtained graphically or using the interpolation method. Based on the experience in calculation, for blade of ordinary size (arc length in the order of several tens mm), it is only necessary to substitute the two integer value in millimeters of  $\Delta y$  near the solution (the approximate value can be estimated easily from the possible shape of the blade) into equation (27) or (28) and then use the linear interpolation method to obtain the solution which is pretty accurate. After the boundary of the duct is known, we can use equation (9) and  $W_m$  as well as its partial derivative value in the y-direction to obtain the velocity distribution on the surface of the blade.

## 2. Compressible Flow

For compressible flow, it is also completely possible to use a similar method as described above to obtain the corresponding equations. As discussed before, at this time we should find the partial derivatives of  $\rho W_x$  and  $W$  in the y-direction and not those of  $W_y$  and  $W_z$  in order to make further calculation more convenient. Equations (23) and (24) are still valid at this time. We also noticed that:

$$\begin{aligned}\frac{\partial(\rho W_x)}{\partial y} &= \rho \frac{\partial W_x}{\partial y} + W_x \frac{\partial \rho}{\partial y} \\ \frac{\partial^2(\rho W_x)}{\partial y^2} &= \rho \frac{\partial^2 W_x}{\partial y^2} + 2 \frac{\partial \rho}{\partial y} \frac{\partial W_x}{\partial y} + W_x \frac{\partial^2 \rho}{\partial y^2} \\ M^2 &= \frac{2}{\gamma - 1} \cdot \frac{W^2}{2c_0 - W^2}\end{aligned}$$

<sup>\*\*</sup> Recently, in Reference [7], it presented a method using the concept of using the flow function to directly calculate  $\Delta y_p$  and  $\Delta y_s$ .

Then from equations (1) ~ (8) after complicated operation, we can obtain the following results:

$$\frac{1}{\rho} \frac{\partial(\rho W_z)}{\partial y} = \left( \frac{\partial W_z}{\partial y} \right)_s - M^2 (B_{14} W \beta' + B_{15} W'') \quad (29)$$

$$\begin{aligned} \frac{1}{\rho} \frac{\partial^2(\rho W_z)}{\partial y^2} = & \left( \frac{\partial^2 W_z}{\partial y^2} \right)_s \\ & + M^2 [B_{15} W B'^2 - 3B_{16} W \beta'' + B_{17} W' \beta' + B_{18} W'' + B_{19} \frac{W'^2}{W}] \\ & + M^4 [(2-\gamma) B_{20} W \beta'^2 + (7-3\gamma) B_{16} W' \beta' - B_{20} W'' + \frac{W'^2}{W} (B_{21} - \gamma B_4)] \\ & - M^4 \gamma B_{20} \frac{W'^2}{W} \end{aligned} \quad (30)$$

$$\frac{\partial W}{\partial y} = \left( \frac{\partial W}{\partial y} \right)_s \quad (31)$$

$$\frac{\partial^2 W}{\partial y^2} = \left( \frac{\partial^2 W}{\partial y^2} \right)_s + M^2 [-B_{10} W' \beta' + B_{13} W''] + M^4 \gamma B_{13} \frac{W'^2}{W} \quad (32)$$

where every B is also a trigonometric function of  $\beta$ . The actual equations can be found in Table 3 in the Appendix.

From here it can be found that, for compressible flow although there are so many terms yet it is also the addition of some simple products. The coefficients of each term can be tabulated in advance (see Table 3 in the Appendix) for use later. Therefore, the computation is also relatively quick and it takes a day or so to complete. The determination of the position of the boundary of the duct at this time can also use the third order algebraic equation and not the numerical integral method:

$$(\rho W_z)_m \Delta y_p + \frac{1}{2} \left[ \frac{\partial(\rho W_z)}{\partial y} \right]_m \Delta y_p^2 + \frac{1}{6} \left[ \frac{\partial^2(\rho W_z)}{\partial y^2} \right]_m \Delta y_p^3 = \frac{1}{2} (\rho W_z)_s \quad (33)$$

$$(\rho W_z)_m \Delta y_s - \frac{1}{2} \left[ \frac{\partial(\rho W_z)}{\partial y} \right]_m \Delta y_s^2 + \frac{1}{6} \left[ \frac{\partial^2(\rho W_z)}{\partial y^2} \right]_m \Delta y_s^3 = \frac{1}{2} (\rho W_z)_s \quad (34)$$

When  $y = y(z)$  is given, the values of  $\beta$ ,  $\beta'$  and  $\beta''$  can be obtained from the following equations:

$$\beta = \tan^{-1}[y'(z)] \quad (35)$$

$$\beta' = \frac{y'}{1+y'^2} = y' \cos^2 \beta = B_1 y' \quad (36)$$

$$\beta'' = \cos^2 \beta (y'' - y'^2 \cdot 2 \cos \beta \sin \beta) = B_1 y'' - 2B_{10} y'^2 \quad (37)$$

Therefore, when some ordinary geometric curves are used as the mean stream line, the equations of each y-direction derivative can also be simplified using the above three equations. Table 2 in the Appendix lists the equations under the special conditions that the mean stream lines are six different curves, respectively. The  $C_1-C_n$ ,  $P_1-P_{10}$ ,  $T_1-T_4$  and  $H_1-H_3$  etc. in the equations are also known trigonometric functions of  $\beta$ . The expressions and values can be looked up in Table 3.

#### IV. Application Examples

In this section, we are using a high subsonic pulsed cascade as an example whose design requires relatively complicated computations. There are many terms to be omitted to simplify the calculation.

The original data of the design are as follows:

Gas Parameters before the Cascade:

stagnation temperature  $T_{0i} = 324^\circ \text{K}$  ,  
 stagnation density  $\rho_{0i} = 1.565 \text{ kg/m}^3$  ,  
 velocity  $W_i = 180 \text{ m/sec}$   
 angle  $\beta_i = 51.2^\circ$  ;

Gas Parameters behind the Cascade:

velocity  $W_e = 264 \text{ m/sec}$   
 angle  $\beta_e = -60^\circ$  ;

The working medium is an ideal gas with  $\gamma = 1.4$  .

The geometric shape of the mean stream line selected in the design: when  $\beta_m > 0$ , it is a circle with radius  $r = 50$  mm. When  $\beta_m < 0$ , it is a suspended chain wave  $y = \eta \cosh(0z) + \lambda$  (mm) where  $\eta = -30.77$  mm,  $0 = 0.0255$  1/mm, and  $\lambda = 80.7$  mm. When the combination of the two types of geometric curves is used as the mean stream line, it is necessary to make sure that the values of  $y_m$ ,  $\beta_m$ ,  $\beta'_m$ , and  $\beta''_m$  are the same on both sides of the junction of the two types of curves. Only by doing so, the results obtained from the above equations will be continuous (when only the first three terms of the Taylor series are used). For ordinary simple geometric curves, this requirement can not be met at any point.

The front and back forehead lines of the cascade are selected right at the places where the  $\beta_m$  of the mean stream line is equal to the given  $\beta_1$  and  $\beta_e$ . For preliminary design, this selection is the only natural choice. But from the discussion in the following section, we can see that this choice should be recommended to be used in general.

The velocity distribution of the mean stream line in this example is selected as follows: When  $\beta_m \geq 0$ , use  $W = \text{constant} = 200$  m/sec. When  $\beta_m < 0$ , then let the velocity increase following a cosine curve to the exit value (270 m/sec), i.e.  $W = 235 - 35 \cos\left(\frac{z}{z_e} \pi\right)$  where  $z_e$  is the value of  $z$  coordinate of the back forehead line of the cascade. Although at  $\beta = 0$   $W$  and  $W'$  are continuous,  $W''$  is not continuous. The continuities of  $W$ ,  $W'$ , and  $W''$  all should be required at the junction point of various velocity variations. But it is generally not easy to achieve. Therefore, for the velocity distribution on the mean stream line in this example, we can imagine the following: When  $\beta_m \geq 0$ , use a constant. When  $\beta_m \leq 10^\circ$ , use the cosine curve as discussed above. As for the segment in the middle,

Table 1. Example of Computation

2 项 目	3 $z$ (毫米)	4 $y$ (毫米)	5 $W$ (米/秒)	6 $W'$ (米/秒·毫米)	7 $W''$ (米/秒·毫米 <sup>2</sup> )	8 $W_2$ (米/秒)
9 公 式	$-r \sin \beta$	$r \cos \beta$	200.0	0.000	0.0000	10 見公式(3)
$\beta = 40^\circ$	-32.14	38.30	200.0	0.000	0.0000	153.2
30°	-25.00	43.30	200.0	0.000	0.0000	173.2
20°	-17.10	46.99	200.0	0.000	0.0000	187.9
10°	- 8.68	49.24	200.0	0.000	0.0000	197.0
0°	0.00	50.00	200.0	0.000	0.0000	200.0
-10°	8.74	49.20	203.6	0.808	0.0860	200.2
-20°	17.60	46.84	213.9	1.457	0.0579	200.7
-30°	26.77	42.54	229.1	1.804	0.0161	198.2
-40°	36.47	35.70	246.6	1.728	-0.0317	188.9
-50°	47.30	24.80	262.5	1.129	-0.0754	168.8
$\beta = -55^\circ$	53.35	16.87	267.9	0.626	-0.0901	153.6
11 公 式	12 按表2第3 行6栏	13 見表2第2 行6栏	$235 - 35 \cos \frac{\pi}{60} z$	$1.831 \sin \frac{\pi}{60} z$	$0.0959 \cos \frac{\pi}{60} z$	14 見公式(3)
15 项 目	16 $z$ (毫米)	17 $y$ (毫米)	18 $W$ (米/秒)	19 $W'$ (米/秒·毫米)	20 $W''$ (米/秒·毫米 <sup>2</sup> )	21 $W_2$ (米/秒)

Table 1 (continued)

(注: 表中已省去下标 m)

$\lambda$	$\rho/\rho_0$	$\rho$ (公斤/米 <sup>3</sup> )	$\rho W_s$ (公斤/米 <sup>2</sup> ·秒)	$M$	$\left(\frac{\partial W_s}{\partial y}\right)_s$ (米/秒·毫米)	$\frac{1}{\rho} \frac{\partial(\rho W_s)}{\partial y}$ (米/秒·毫米)
$\frac{W}{\sqrt{\frac{2\gamma}{\gamma+1} K T_{0i}}}$	按 $\lambda$ 查气 动函数表 26	$\rho_{0i} \left(\frac{\rho}{\rho_0}\right)$	$\rho \cdot W_s$	按 $\lambda$ 查气 动函数表 27	见表 2 第 6 行 第 2 栏 28	见表 2 第 10 行 第 2 栏 29
0.606	0.855	1.339	205.0	0.571	-0.694	0.0716
0.606	0.855	1.339	232.0	0.571	-2.000	-1.021
0.606	0.655	1.339	251.5	0.571	-3.064	-1.913
0.606	0.855	1.339	263.5	0.571	-3.759	-2.494
0.606	0.855	1.339	267.8	0.571	-4.000	-2.696
0.617	0.849	1.330	266.0	0.582	-4.019	-2.616
0.648	0.835	1.308	262.7	0.613	-3.876	-2.247
0.694	0.811	1.271	252.0	0.661	-3.201	-1.400
0.747	0.783	1.226	231.5	0.716	-1.864	-0.222
0.795	0.757	1.186	200.2	0.768	-0.274	0.766
0.811	0.747	1.171	179.8	0.785	+0.380	1.007
$\frac{W}{\sqrt{\frac{2\gamma}{\gamma+1} K T_{0i}}}$	按 $\lambda$ 查气 动函数表 30	$\rho_{0i} \left(\frac{\rho}{\rho_0}\right)$	$\rho \cdot W_s$	按 $\lambda$ 查气 动函数表 31	见表 2 第 6 行 第 6 栏 32	见表 2 第 10 行 第 6 栏 33
$\lambda$	$\rho/\rho_0$	$\rho$ (公斤/米 <sup>3</sup> )	$\rho W_s$ (公斤/米 <sup>2</sup> ·秒)	$M$	$\left(\frac{\partial W_s}{\partial y}\right)_s$ (米/秒·毫米)	$\frac{1}{\rho} \frac{\partial(\rho W_s)}{\partial y}$ (米/秒·毫米)

Table 1 (continued)

项 目	$\left(\frac{\partial^2 W'}{\partial y^2}\right)_B$ (米/秒·毫米 <sup>2</sup> )	$\frac{1}{\rho} \frac{\partial^2 (\rho W')}{\partial y^2}$ (米/秒·毫米 <sup>2</sup> )	$\frac{\partial W'}{\partial y}$ (米/秒·毫米)	$\left(\frac{\partial^2 W'}{\partial y^2}\right)_B$ (米/秒·毫米 <sup>2</sup> )	$\frac{\partial^2 W'}{\partial y^2}$ (米/秒·毫米 <sup>2</sup> )
公 式	见表 2 第 7 行 第 2 栏	见表 2 第 11 行 第 2 栏	见表 2 第 8 行 第 2 栏	见表 2 第 9 行 第 2 栏	见表 2 第 12 行 第 2 栏
$\beta = 40^\circ$	-0.0800	-0.1116	-3.064	0.0608	0.0608
30°	0.0000	-0.0645	-3.464	0.1000	0.1000
20°	0.0800	-0.0155	-3.759	0.1320	0.1320
10°	0.1387	0.0214	-3.939	0.1528	0.1528
0°	0.1600	0.0346	-4.000	0.1600	0.1600
-10°	0.0792	-0.0104	-4.065	0.0808	0.1078
-20°	0.0820	-0.0347	-4.145	0.1008	0.1163
-30°	0.0206	-0.0886	-3.983	0.0799	0.0812
-40°	-0.0673	-0.1264	-3.326	0.0163	0.0079
-50°	-0.0927	-0.0668	-2.186	-0.0385	-0.0477
$\beta = -55^\circ$	-0.0734	-0.0361	-1.498	-0.0472	-0.0340
公 式	见表 2 第 7 行 第 6 栏	见表 2 第 11 行 第 6 栏	见表 2 第 8 行 第 6 栏	见表 2 第 9 行 第 6 栏	见表 2 第 12 行 第 6 栏
项 目	$\left(\frac{\partial^2 W'}{\partial y^2}\right)_B$ (米/秒·毫米 <sup>2</sup> )	$\frac{1}{\rho} \frac{\partial^2 (\rho W')}{\partial y^2}$ (米/秒·毫米 <sup>2</sup> )	$\frac{\partial W'}{\partial y}$ (米/秒·毫米)	$\left(\frac{\partial^2 W'}{\partial y^2}\right)_B$ (米/秒·毫米 <sup>2</sup> )	$\frac{\partial^2 W'}{\partial y^2}$ (米/秒·毫米 <sup>2</sup> )

Table 1 (continued)

$\Delta y_p$ (mm)	$\Delta y_s$ (mm)	$y_p$ (mm)	$y_s$ (mm)	$w_p$ (m/sec)	$w_s$ (m/sec)
see eq. (33)	see eq. (34)	$y_m + \Delta y_p$	$y_m - \Delta y_s$	<sup>48</sup> 用公式(9)前3项	<sup>49</sup> 用公式(9)前3项
22.17	23.08	61.08	15.22	146.1	286.9
20.83	18.36	64.13	24.94	149.6	280.6
19.55	16.21	66.54	30.78	151.8	278.3
18.82	15.17	68.06	34.07	153.0	277.3
18.61	14.88	68.61	35.12	153.3	277.2
18.96	15.19	68.16	34.01	146.5	277.3
18.92	15.49	65.76	31.35	156.3	292.0
19.32	16.82	61.86	25.72	167.4	307.6
20.16	19.59	55.86	16.11	180.2	313.1
21.59	24.26	46.39	0.54	204.3	301.5
23.21	27.87	40.08	-11.00	218.6	288.7
see eq. (33)	see eq. (34)	$y_m + \Delta y_p$	$y_m - \Delta y_s$	<sup>50</sup> 用公式(9)前3项	<sup>51</sup> 用公式(9)前3项
$\Delta y_p$ (mm)	$\Delta y_s$ (mm)	$y_p$ (mm)	$y_s$ (mm)	$w_p$ (m/sec)	$w_s$ (m/sec)



Key to Table 1: 2. item, 3.  $z(\text{mm})$ , 4.  $y(\text{mm})$ , 5.  $w(\text{m/sec})$ ,  
6.  $W'(\text{m/sec.mm})$ , 7.  $W''(\text{M/sec mm}^2)$ , 8.  $W_z(\text{m/sec})$ , 9. equation,  
10. see equation (3), 11. equation, 12. Based on 6th column  
of the 3rd line in Table 2, 13. Based on 6th column of the  
2nd line in Table 2, 14. see equation (3), 15. item, 16.  $z(\text{mm})$ ,  
17.  $y(\text{mm})$ , 18.  $W(\text{m/sec})$ , 19.  $W'(\text{m/sec.mm})$ , 20.  $W''(\text{m/sec.mm}^2)$ ,  
21.  $W_z(\text{m/sec})$ , 22.  $p(\text{kg/m}^3)$ , 23.  $(\text{kg/m}^2 \text{ sec})$ , 24.  $(\text{m/sec.mm})$ ,  
25.  $(\text{M/sec.mm})$ , 26. look up the table of aerodynamic functions  
based on  $\lambda$ , 27. look up the table of aerodynamic functions  
based on  $\lambda$ , 28. see the 2nd column in line 6 in Table 2, 29.  
see the 2nd column in line 10 in Table 2, 30. look up the  
table of aerodynamic functions based on  $\lambda$ , 31. look up the  
table of aerodynamic functions based on  $\lambda$ , 32. see the 6th  
column in line 6 in Table 2, 33. see the 6th column in line  
10 in Table 2.  
34.  $p(\text{Kg/m}^3)$ , 35.  $pW_z(\text{Kg/m}^2 \text{ sec})$ , 36.  $(\text{M/sec.mm})$ , 37.  $\text{M/sec.mm})$   
38. see col. 2 of line 7 in Table 2, 39. see col. 2 of line 11  
in Table 2, 40. see col. 2 of line 8 in Table 2, 41. see col.  
2 of line 9 in Table 2, 42. see col. 2 of line 12 in Table 2,  
43. see col. 6 of line 7 in Table 2, 44. see col. 6 of line 11  
in Table 2, 45. see col. 6 of line 8 in Table 2, 46. see col.  
6 of line 9 in Table 2, 47. see col. 6 of line 12 in Table 2  
48. use the first 3 terms of equation (9), 49. use the first  
3 terms of equation (9), 50. use the first 3 terms of equation  
(9), 51. use the first 3 terms of equation (9)

a higher order of smooth curve is used as the transition. Because the calculation points are always finite and discrete, therefore the transition condition in between calculation points can have some degree of arbitrariness.\* By how much the velocities at the entrance and exit on the mean stream line are greater than the given velocity values in the front and the back of the cascade, by how much the value of  $Ph$ , at the corresponding point is greater than the given values in front and at the back of the cascade, also determines the extent of dullness at the front fringe of the blade.<sup>[1]</sup> The M number in this example is large, therefore, a sharper design is used in order to avoid a partial supersonic effect at the entrance.

The cascade distance in this example is 56.4 mm corresponding to a cascade density of 1.8.

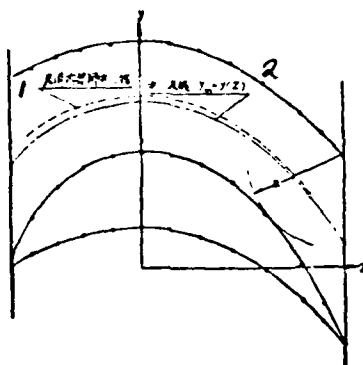
The computational results and procedures are shown in Table 1 and Figures 2 and 3. From the calculated results, it can be found that the coordinates of points on the surface of the blade shape obtained using the analytical solution of the mean stream line method are completely smooth. It is much smoother than the solution obtained using the numerical method (for example) refer to Reference [3]). This also indicates that the accuracy of the solution is correspondingly higher. Naturally, as described above, the speed of calculation is also much faster.

For the design of a cascade, the blade profile obtained in this example can be considered to be satisfactory: even when the M number near the exit reaches 0.8, there is no supersonic region in the entire duct. There is even some margin (the maximum M number on the back arc of the blade profile

\* The discontinuity of  $w$  at the junction still has some effect on the smoothness of the calculated results. For example, the variation of  $\Delta y_p$  in the region where  $\beta = 6 \sim 20^\circ$  is not most ideal.

But the effect is small and the surface of the blade is still smooth.

is about 0.94). The velocity distribution on the entire blade is also satisfactory. The variation is uniform ( $W_{max}/W_{min} = 1.15$ ). The compression gradient in the compression region which exists in the exit section of the back arc of an ordinary cascade is not large. This indicates that the use of the method presented in this paper to design good planar cascades is completely possible.



• 計算所得座标点 3

Figure 2. The schematic of the blade profile obtained from the sample calculation  $\beta_i = 51.2^\circ$ ,  $\beta_e = -60^\circ$ ,  $\lambda_e = 0.8$ .

Key: 1. mean line of the inner contact circle inside the duct, 2. mean stream line  $y_m = y(z)$ , 3. coordination points obtained from calculation.

$$\left( \frac{h}{t} = 1.83, \frac{\delta_{max}}{B} = 0.232, \frac{a}{B} = 0.394 \right)$$

As for the gas exit angle, we can use the following empirical equation from the designed black profile to verify:

$$\beta_e = \cos^{-1} \frac{a}{t} \quad (38)$$

where  $a$  is the width at the throat of the outlet of the duct (see Figure 2). The obtained result is  $\beta_e = 60.2^\circ$ . It is basically consistent with the design requirement.

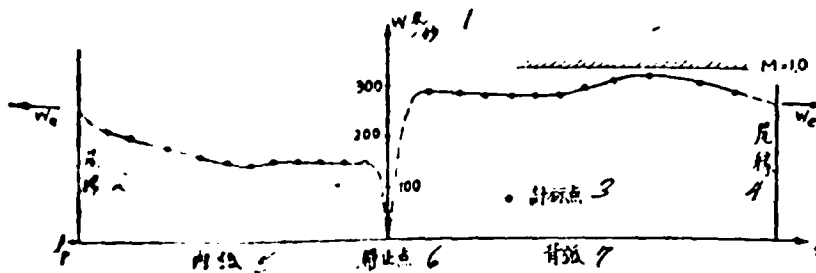


Figure 2. Velocity distribution on the blade profile obtained from the sample calculation.

Key: 1. leading edge, 2. near fringe, 3. calculated point, 4. rear fringe, 5. inner arc, 6. stagnation point, 7. back arc,

#### V. The Selection of Variation of the Design Variables

As described above, when using the mean stream line method to design planar cascades, the design variables can be chosen are the shape of the mean stream line and the velocity distribution on it (which includes the choices of the points on that stream line that intersect with the front and back forehead lines and by how much the velocities at those points are greater than the given velocity values in the front and back of the cascade). Whether a good cascade can be designed, the problem lies on the proper selection of these design variables.

In order to acquire some preliminary experience in designing, we have carried out many design calculations for various types of blade profiles from different shapes of mean stream lines and various velocity distributions on the mean stream line. Because the solutions to the reverse problem of the subsonic compressible flow is qualitatively very close to that of the incompressible flow, therefore during the calculations most of the time we use the incompressible flow in order

to obtain more information for comparison more conveniently. The following is a presentation of preliminary recommendations on the selection of design parameters based on the meaningful results obtained from the information already in hand.

### 1. Pulsed Cascade

In the calculation, a comparison is carried out on the different velocity distributions of pulsed blade family with a circular mean stream line. The result obtained is: Regardless of whether the flow is compressible or incompressible and the distribution of velocity on the mean stream line (as long as the variation is not too large), the trend of variation of the velocity distribution on both sides of the duct (that is on both sides of the blade) is similar to that of the velocity distribution on the mean stream line. This results can be qualitatively explained as: because the curvature of a circle is uniform everywhere, therefore the difference of the velocity at the boundaries of the duct is not too different from that on the mean stream line. The typical conditions can be seen in Figures 4 and 5\*.

From these two figures, it is easy to find out that the aerodynamic property is not good for the blade profile using a circular arc as the entire mean stream line. Because that the velocity distribution of the back arc is basically parallel to that on the mean stream line, in the segment near the outlet

\*For the convenience of referring to the blade, the velocity distribution is plotted along the  $z$  direction rather than along the surface of the blade profile starting from Figure 4. Thus the absolute value of the gradient of velocity appears larger in the front and back fringes - especially at the rear fringe of the back arc. The actual velocity gradient  $\left| \frac{\partial u}{\partial x} \right|$  is actually much small. Please notice this point when referring to all figures afterwards.

on the back arc of the blade there must be violent compression and gas separation caused by it. In the internal combustion turbine laboratory of Tsung hua University, we have carried out a low velocity wind tunnel experiment on the planar cascade basically similar to the design shown in Figure 4. The result showed that there is a separation region at the exit of the back arc of the blade. The flow field behind the cascade is extremely inhomogeneous.

When placing colored liquid in the separation region on the back arc, we can use our naked eyes to observe the appearance of whirlpools in this region. The liquid droplets adhere to the blade in rotation and do not get blown away. These indicate that the design using circular arc as the entire mean stream line is not good.

But for ordinary pulsed cascades, the velocity variation in front and behind the cascade is not large. It is naturally proper to have less variation in the velocity distribution on the mean stream line. There is not too much choice. The velocity distribution on the back arc at this time is usually desired to be flat and invariant at the beginning and then it is followed by a segment of compression region with a velocity gradient of a negative value which is not too large and finally connects to the value of the exit velocity. Therefore, for the beginning section of the duct in a pulsed cascade, the use of a circular arc as the mean stream line and taking the value of the velocity as a constant are recommended. At this time the rising section of the back arc has a basically flat distribution of velocity. After that we can find some curves as the mean stream line to satisfy the latter requirement discussed above.

In order to compare the effect of the shape of the mean

stream line more conveniently, the blade profiles of three types of mean stream lines with constant velocity distribution are shown in Figures 6, 7, and 8. The first halves ( $\beta_m > 0$ ) of the mean stream lines are all circular arcs and the rear halves ( $\beta_m < 0$ ) are equi-angular variation curve in the  $z$  direction (its analytical equation can be found in Table 2 of the Appendix), suspended chain curve, and parabolic curve, respectively. The junction point of various mean stream lines is fixed at  $\beta_m = 0$  because only here it is convenient to make the variations of  $r_m$ ,  $\beta_m$ ,  $\beta'_m$  and  $\beta''_m$  continuous.

From these three figures, we can see that in the latter half of the duct where  $\beta_m < 0$ , the effect of velocity distribution on the back arc for the three mean stream lines is different. When the mean stream line is a parabolic curve, the velocity on the back arc initially drops rapidly and then gradually flattens out. In the case of the suspended chain curve, the situation is the uniformly compression along the  $z$  direction. In the case of the equi-angular variation curve in the  $z$  direction, the compression region is more concentrated towards the rear (but as discussed above, the velocity distribution is plotted in the  $z$  direction. When transformed into a plot along the surface of the blade, due to the higher deviation away from the axial direction in the rear of the blade, the negative value of the velocity gradient is not too large). If the circular arc is also used as the mean stream line in the  $\beta_m < 0$  region, then we will obtain situations in which the compression region is concentrated even more towards the rear. The velocity value on the back arc is basically the constant. Only in a very short section near the outlet violent compression occurs. From these four conditions, it seems that it is related to the variation of the  $\beta'_m$  value (the corresponding curvature) on their mean stream lines after  $\beta_m < 0$  (refer to Table 2 in the Appendix). The  $\beta'_m$  of the equi- $z$ -directional angular variation

curve in the z direction is a constant. The absolute value of

$\beta'_m = 0^1 (v_m - \lambda) \cos^2 \beta_m$  for a suspended chain curve is becoming smaller in the z-direction (the absolute value of the term  $(v_m - \lambda)$  is getting larger, the term  $\cos^2 \beta_m$  is getting smaller, but the latter is the dominant factor), its initial compression this arrives faster. The absolute value of  $\beta'_m = 2 \eta \cos^2 \beta_m$  for the parabolic curve becomes smaller even faster, therefore, the compression begins even more rapidly. On the contrary, the absolute value of  $\beta'_m = -\frac{1}{r} \cdot \frac{1}{\cos \beta_m}$  for a circular arc in the z direction is getting larger when  $\beta_m < 0$ . The onset of its compression then is slower than that of the equi-z-directional angular variation curve. The effect of using other ordinary curve as the mean stream line can also be evaluated approximately based on this technique.

From the above figures, it can be found that for pulsed cascades we can recommend a circle when  $\beta_m < 0$  and an equi-z-directional angular variation curve or a suspended chain curve when  $\beta_m < 0$  as the mean stream line. The choice between the two latter ones should take the application condition of the cascade into consideration. If the estimation shows that the velocity distribution of the former will not cause separation, then it is better to use the equi-z-directional angular variation curve because the density can be reduced for the same cascade distance, the width of the blade can also be decreased, and the frictional loss of flow can be minimized.

As discussed above, for pulsed cascades, there is not too much choice in the velocity distribution or the mean stream line. If the M number is not too large, we can directly choose the velocity distribution on the mean stream line as a straight line or as a constant. If the maximum velocity is to be reduced and the compression gradient is to be minimized to the extent possible, then we can first choose the lowest possible



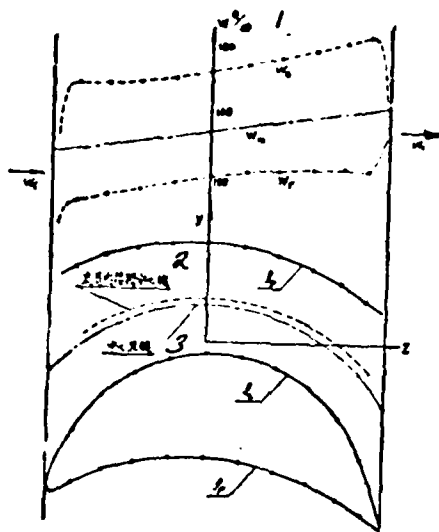


Fig. 4. The blade profile and velocity distribution when the mean stream line is a circle.

$$(M_0 = 0, \beta_i = 50^\circ, \beta_r = -60^\circ, \frac{W_{r, \max}}{W_0} = 1.45, \frac{b}{s} = 1.54, \frac{\delta_{\max}}{B} = 0.32, \frac{\pi}{B} = 0.47)$$

Key: 1. W m/sec, 2. center line of the inner contact circle of the duct, 3. mean stream line.

constant as the velocity on the mean stream line and then use a certain curve to connect to the value at the rear fringe (its selection will be shown later). For example, it has been done this way in the above example. Another example is shown in Figure 9. The given parameters, the shape of the mean stream line, and the selection of the cascade distance of this blade profile are the same as those in Figure 7. Only the velocity distribution on the mean stream line is different. Comparing these two examples, we can see the effect of this change.

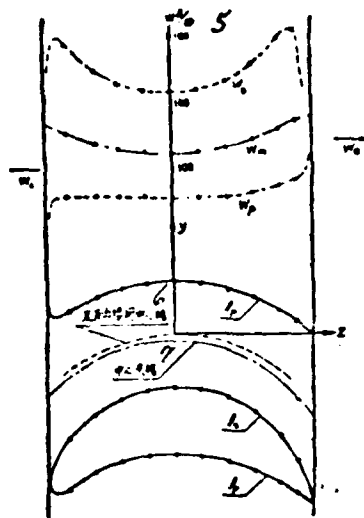


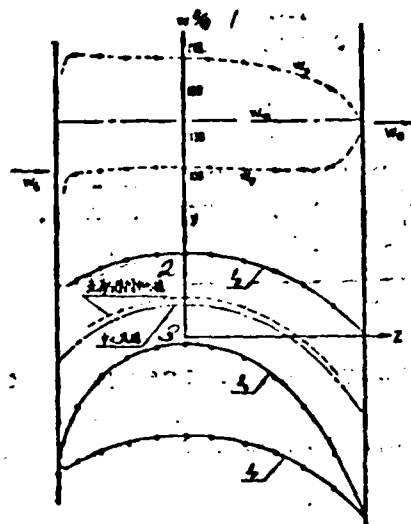
Fig. 5. The blade profile and velocity distribution when the mean stream line is a circle.

$$(M_0=0.2, \beta_1=50^\circ, \beta_2=-55.2^\circ, \frac{w_{1max}}{w_0} = 1.59, \frac{b}{l} = 1.53, \frac{\delta_{max}}{B} = 0.255, \frac{\eta}{B} = 0.50)$$

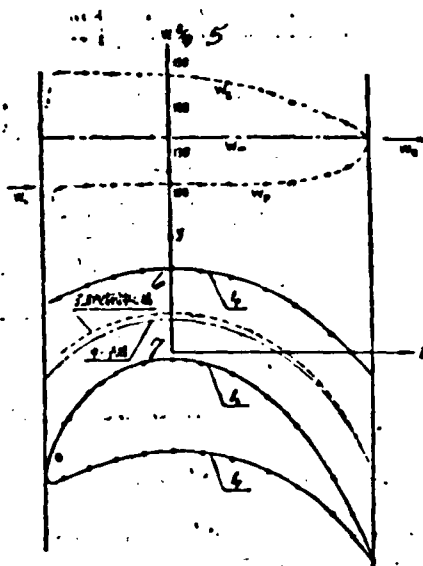
Key: 5.  $w$  m/sec, 6. center line of the inner contact circle of the duct, 7. mean stream line.

## 2. Reversed Cascade

There is little experience in using the mean stream line method to design the reversed blade profiles<sup>[3]</sup>. Since the mean stream line and the velocity distribution on it are simultaneously affecting it more significantly, it is then more difficult to analyze the effects. But we can be sure that the qualitative effect of the mean stream line as discussed above is still approximately correct. For the comparison of the effect of velocity distribution on the mean stream line at this time, Figures 10, 11, and 12 show the results of three blade profile designs with different velocity distributions on the mean stream line. (They are a straight line  $w_m = w_0 + \eta_1 z$ , a second order parabolic curve  $w_m = w_0 - \eta_2 z + \eta_3 z^2$ , and an eighth order polynomial  $w_m = w_0 + \eta_4 z + \eta_5 z^2$ , respectively). but the other parameters remained the same. It is apparent that, for the reversed cascade, the velocity gradient on the



$$(M_0 = 0, \beta_1 = 50^\circ, \beta_2 = -60^\circ, \frac{W_{f, \max}}{W_0} = 1.43, \frac{b}{t} = 1.67, \frac{\delta_{\max}}{B} = 0.305, \frac{u}{B} = 0.421)$$



$$(M_0 = 0, \beta_1 = 50^\circ, \beta_2 = -60^\circ, \frac{W_{f, \max}}{W_0} = 1.43, \frac{b}{t} = 1.85, \frac{\delta_{\max}}{B} = 0.281, \frac{u}{B} = 0.392)$$

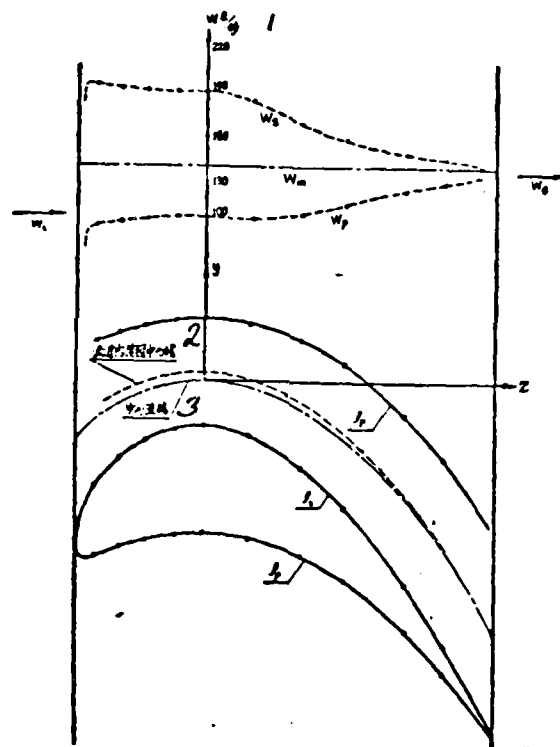
Figure 6. The blade profile and velocity distribution when the mean stream line is a circle ( $\beta_m > 0$ ) and an equi-z-directional angular variation curve ( $\beta_m < 0$ ).

Key: 1.  $W$  m/sec, 2. center line of the inner contact circle of the duct, 3. mean stream line.

Figure 7. The blade profile and velocity distribution when the mean stream line is a circle ( $\beta_m > 0$ ) and a suspended chain curve ( $\beta_m < 0$ ). Key: 5.  $W$  m/sec, 6. center line of the inner contact circle of the duct, 7. mean stream line.

mean stream line is generally positive. From these three figures and some computational results, we found that: in order to make the compression small in the most troublesome area near the rear fringe of the back arc, we should choose the smallest  $W_m'$  value at that place possible.  $W_m''$  is a negative number ( $W_m$  may be relatively larger at this time)

as shown in Figures 3 and 12. We should not use the smallest  $W_m$  possible in front of the rear fringe as we might have imagined. It would rapidly become larger as shown in Figure 11. Besides, we must also realize that, at the front and rear fringes, in addition to  $W_m$  the values of  $W_m'$  are also influencing the thickness of the front and rear fringes significantly. The front (rear) fringe has a larger  $W_m'$  than it makes the from (rear) fringe thicker. This can be found by comparing the blade profiles in Figures 10 ~ 12.



$$(M_e = 0, \beta_e = 50^\circ, \beta_e = -60^\circ, \frac{W_{s,max}}{W_e} = 1.51, \frac{b}{t} = 2.13, \frac{\delta_{max}}{B} = 0.26, \frac{n}{B} = 0.306)$$

Figure 8. The blade profile and the velocity distribution of a mean stream line which is a circle when ( $\beta_m > 0$ ) and a parabolic curve when ( $\beta_m < 0$ ). Key: 1.  $W$  m/sec, 2. center line of the inner contact circle of the duct, 3. mean stream line.

Just as pointed out in Reference [3], in the design of reversed blade profile, it is more appropriate to use the stream line which has 60% of the flow away from the back arc as the mean stream line. When the analytical method is used to carry out the design work, the same experience has been verified. In addition to the fact that the mean stream line is farther away from the inner arc as pointed out in Reference [3], this is also due to the better convergence towards the back arc direction when using Taylor series to expand  $\rho W$ .

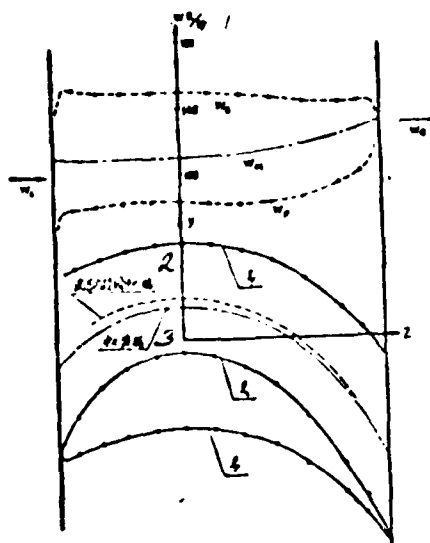
Therefore, in the design of blade profiles of the reversed type, it is recommended to use the 60% stream line of an equi-z-directional angular variation curve or a suspended chain curve. The velocity distribution on the stream line should be the type which increases uniformly and becomes flat at the rear fringe for better results. Another example of blade profile with this type of design can be seen in Figure 13.

After the mean stream line is selected, as described above, there is still this problem left to determine the positions of the front and rear fringes. The difficulty to precisely obtain the shapes of the front and rear fringes to satisfy the requirements of entrance and exit angles of the gas is one disadvantage of the mean stream line method. But based on the experience acquired from calculations, it should be recommended to take the position of the rear fringe at  $\beta_m = \beta_e$ . The value of  $\cos^{-1} \frac{u}{V}$  at this time is very close to that of  $\beta_e$ . For all the calculations, it is within  $\pm 2^\circ$ . If the gas exit angle of the black profile must be changed by  $\pm \Delta\beta$  in order to satisfy a requirement after the design work is completed, then it is recommended to preliminarily change the  $\beta_m$  by  $\pm \Delta\beta$  at the rear fringe as an approximation. Of course, we can also find the exit angle of the gas from the

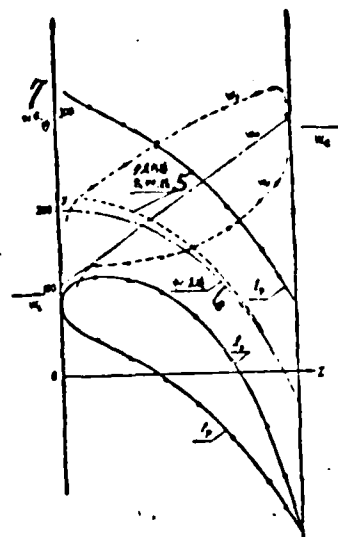
momentum variation in the duct based on the velocity distribution. But because the velocity distributions at the front and the rear fringes can not be obtained accurately at the present time, it is still very difficult to accurately determine the exit angle of the gas using this method. The position of the front fringe can be generally taken at  $\beta_m = \beta_i$ . This is more appropriate for the pulsed cascades. Because of the larger gas entrance angle  $\beta_i$  at that time, the deviation of the incoming flow by the cascade is smaller<sup>[4]</sup>. In addition, since the mean stream line is located at the center of the duct, the circular components of the deviation due to blades on both sides can easily cancel each other. Besides, for pulsed cascades which are denser, the slight change in the gas entrance angle only affects the area near the front fringe. The effect on the velocity distribution of the entire blade profile is very small<sup>[5]</sup>. Even if there is some deviation, it does not matter that much. For reversed cascades, the position of the front fringe can be taken as  $\beta_m = \beta_i + \Delta\beta$  where  $\Delta\beta$  can be  $0^\circ \sim 10^\circ$  preliminarily. When the gas entrance angle  $\beta_i$  is smaller, then  $\Delta\beta$  must be larger<sup>[4]</sup>.

In the selection of the velocity distribution on the mean stream line, the  $W_m$  values at the front and back fringes are major factors which determine the thicknesses at the front and back fringes. For conventional blade profiles, it is recommended to take  $W_m = (1.10 \sim 1.35)W_c$  at the front fringe and  $W_m = (1.02 \sim 1.08)W_c$  at the rear fringe. Naturally, a large value of  $W_m$  should be used at the front or rear fringe when thicker fringes are desired. In addition, the effect of  $W_m'$  as discussed above should also be considered.

In the design of the cascades, the selection of cascade distance can be made by referring to the existing cascade data. But if the distance used is too large, it may not be possible



$$(M_e = 0, \beta_i = 50^\circ, \beta_e = -60^\circ, \frac{W_e^{\max}}{W_e} = 1.19, \frac{b}{t} = 1.81, \frac{\delta_{\max}}{B} = 0.234, \frac{n}{B} = 0.391)$$



$$(M_e = 0, \beta_i = 0^\circ, \beta_e = -70^\circ, \frac{W_e^{\max}}{W_e} = 1.16, \frac{b}{t} = 1.43, \frac{\delta_{\max}}{B} = 0.38, \frac{n}{B} = 0.50)$$

Figure 9. The blade profile and velocity distribution of the mean stream line which is a circle ( $\beta_m > 0$ ) and a suspended chain curve ( $\beta_m < 0$ ). Key: 1.  $W$  m/sec, 2. center line of the inner contact circle in the duct, 3. mean stream line.

Figure 10. The reversed type blade profile and velocity distribution of the mean stream line which is an equi- $z$ -directional angular variation curve. Key: 5. center line of the inner contact circle in the duct, 6. mean stream line, 7.  $M$  m/sec.

to use only the first three terms of the Taylor series in the mean stream line method. This can be realized by noticing a rapid change of  $PW$ , in the  $y$  direction (usually the fact that it becomes smaller near the inner arc shows up first) when calculating equations (33) and (34). Therefore, in the present use of the mean stream line method to design planar turbine cascades, it is more appropriate to choose a cascade density greater than 1.4

As discussed above, the solutions of the blade profiles of the subsonic compressible flow and incompressible flow are

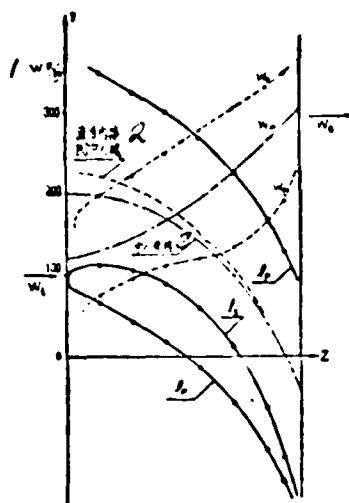
very close. With the same mean stream line, basically it only shifts the blade profile towards the direction of the inner arc. (Strictly speaking it is impossible to compare between the two cases. This is because that the velocity distribution on the mean stream line cannot be the same for the compressible and incompressible cases when the mean stream lines are the same. Similarly, at  $W_1$  the compressible  $W_e$  is larger, therefore, the velocity distribution values of the blade profile obtained are also larger). In addition, because of the variation in density, when the  $W_m$  of the front (or rear) fringe is greater or equal to that of  $W_1$  or  $W_e$ , the increase of  $PW$ , for the compressible case is smaller which means that the front (or rear) fringe can be made thinner. However, this effect is not significant. Besides these, we can imagine that: in the subsonic region, it may be more accurate to use the mean stream line method when the M number is larger. This is because that the trends of variation of  $W_z$  and  $\rho$  are opposite where using Taylor series expansion on both sides. Thus it makes it possible that the series of  $PW$ , may converge more rapidly.

#### IV. The Design Method Which Satisfies a Given Blade Thickness Distribution

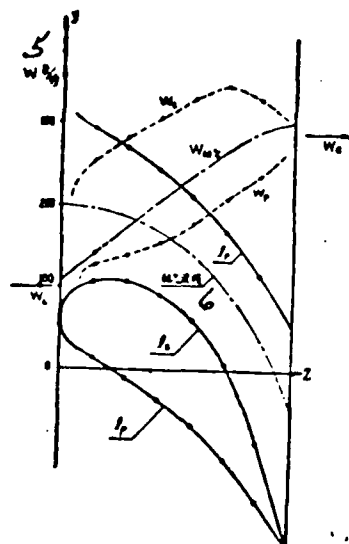
The next advantage of the mean stream line method is that it allows the design of a blade profile which approximately satisfies a preset thickness distribution in order to ensure the strength, rigidity and cooling requirements of the blades [1]. When using the analytical method to carry out the calculation, there are two design methods to assure the thickness distribution as discussed in the following.

In one of the two methods, the design variables are still  $y_m = y(z)$  and  $W_m = W(z)$  as discussed before. In order to assure the distribution of thickness at this time, we





$$(M_e = 0, \beta_i = 0^\circ, \beta_e = -70^\circ, \frac{W_{e, \max}}{W_e} = 1.19, \frac{b}{t} = 1.43, \frac{\delta_{\max}}{B} = 0.265, \frac{\pi}{B} = 0.57)$$



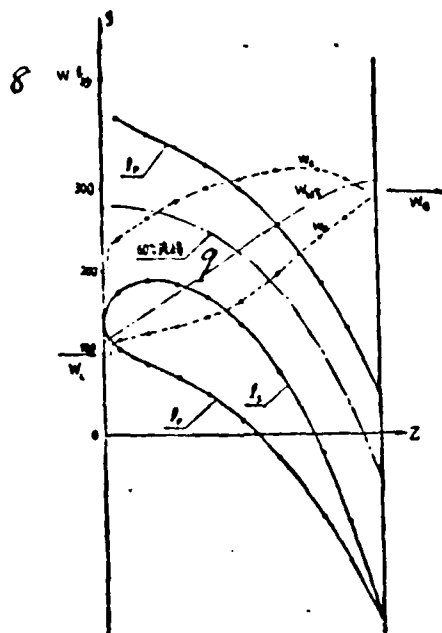
$$(M_e = 0, \beta_i = 0^\circ, \beta_e = -70^\circ, \frac{W_{e, \max}}{W_e} = 1.10, \frac{b}{t} = 1.43, \frac{\delta_{\max}}{B} = 0.46, \frac{\pi}{B} = 0.53)$$

Figure 11. The reversed type blade profile and velocity distribution when the mean stream line is an equi-z-directional angular variation curve.  
Key: 1. W m/sec, 2. center line of the inner contact circle in the duct, 3. mean stream line.

Figure 12. The reversed type blade profile and velocity distribution when the mean stream line is an equi-z-directional angular variation curve.  
Key: 5. W m/sec, 6. 60°/stream line.

should follow the instructions in Reference [1] to initially assume that  $(PIV_z)_m^* = t/t - \delta$  to determine the approximate variational curve  $(PIV_z)_m \sim z$ . After the shape of the mean stream line  $y_m = y(z)$  is selected, the variation curve  $W_m \sim z$  can be obtained from the first order isentropic aerodynamic equation. That means we can use an analytical expression

$W_m = W(z)$  which is very similar to this curve to replace it to solve the problem. Since the relation between  $(PIV_z)_m^*$  and  $t/t - \delta$  is already very similar and the thickness distribution of the blade in actual design work only has to satisfy the



$$(M_e = 0, \beta_1 = 0^\circ, \beta_e = -70^\circ, \frac{W_{e, \max}}{W_e} = 1.10, \\ \frac{b}{l} = 1.79, \frac{\delta_{\max}}{B} = 0.364, \frac{\eta}{B} = 0.43)$$

Figure 13. The reversed type blade profile and velocity distribution of the mean stream line which is a suspended chain curve.

Key: 8.  $W$  m/sec, 9. 60% stream line.

requirements approximately, therefore it does not have to be too rigorous to transform  $(PW_z)_m \sim z$  into  $W_m \sim z$  and finally onto  $W_m = W(z)$  in order to avoid mathematical difficulties and increase the computational speed.

The other method also used the selection of  $(PW_z)_m = \omega(z)$  and  $y_m = y(z)$  as in Reference [1] to be the variables in order to obtain a series of equations from which the analytical solution can be found. Their forms are very similar to the ones given in Section III of this paper. Since in the actual design it does not require the strict assurance of the thickness distribution, we can use the approximately corresponding

$W_{z,m} = W_z(z)$  to replace  $(PW_z)_m = \omega(z)$  as the variable. The actual equations are omitted here to save space. It has been documented in detail in Reference [8].

## VII. Solving the Forward Problem Using the Analytical Method

It is more complicated to solve the forward problem using the analytical method because it is necessary to find the analytical expressions  $W_m = W(z)$  and  $v_m = v(z)$  which satisfy the boundary of the blade profile at this time. However, it still has some advantages over the numerical differentiation method used in the past. Since it is unavoidable to carry out a few trial runs to approach the boundary of the blade profile in solving the forward problem<sup>[1], [3]</sup>, it is of course more convenient and fast to perform these trial runs using the analytical method. From this we can first obtain the mean stream line and the trend of variation of parameters on it. We then can use the numerical solution to make the final correction. Thus the entire approaching processes can be completed faster and more accurately. Actually for those who are already familiar with the analytical method, it is more desirable to use the analytical method to carry out the entire approaching process. Based on the experience acquired to date, it is not going to be slower than using the numerical method. Since it avoids numerical differentiations, the accuracy is even higher.

Because that the accuracy in using the analytical method to solve the reverse problem is higher and there are lots of calculated blade profiles available to be referred to, therefore we have verified these blade profiles in order to examine the validity of the empirical variational rules of  $v_m \sim z$  and  $(\rho W_z)_m \sim z$  as presented in References [1] and [3]. The result of verification is satisfactory. We can only supplement as follows: the position of the mean stream line for an incompressible flow is even more toward the inner arc than the one obtained using the plotting method in Reference [3] (the physical meaning of this point is obvious). We suggest that the envelop curve  $aa'b$  in Figure 5 of Reference

[3] be used directly as the mean stream line\*. In addition, under many conditions there are similarities between the  $(PIV)_m^*$  curve and the  $\cos\beta/D \sim$  curve (specific situations are shown in Reference [8]). Therefore, in solving the forward problem using the analytical method, it is possible to use these recommended analytical expressions which are determined to have approximately the same variations as  $y_m$  and  $(PIV)_m^*$  or  $(PIV)_m^*$  to obtain the preliminary solution. When the obtained duct boundary is not consistent with the given condition, we can carry out a correction as presented in References [1] and [3], and then list the analytical expressions after the correction. If one is familiar with the characteristics of various curves, it is not a difficult step either. As discussed above, in the selection of the analytical expressions of  $w_m$  and  $(PIV)_m^*$  or  $w_m^*$ , it is possible to connect them with several curves which is more convenient in finding the solution to the forward problem. If it is difficult to make  $w_m, w'_m, w''_m$  and  $y_m, \beta_m, \beta'_m, \beta''_m$  continuous at the junction, it is also possible to separate the defined region by assuming that another segment of a smooth curve is connecting them.

#### VIII. Accuracy of the Analytical Method

The mean stream line method has already been verified experimentally. This paper merely presents an improvement in the specific calculation procedure. It does not alter its conditions and simplification assumptions. Therefore, it is not necessary to conduct another experimental verification. However, for the further verification of the reliability, the speed of solving the forward problem, and the applicability to the compressor cascades, we have carried out the forward

\* Comrade Wei Yu Ping who is a graduate student of Tsing Hua University Internal Combustion Machinery Group has participated in this verification work.

problem calculation using the analytical method on the two cascades with experimental data shown in References [4] and [6]. The comparison of calculated and experimental results are shown in Figures 14 and 15. The former corresponds to a cascade with the second series of original black profile in Reference [4] with  $\beta_1 = 60^\circ$ , attack angle (angle between  $W_1$  and the line of the arc) is  $75^\circ$ , the center line deflection angle of the blade profile is  $120^\circ$ , and the density is 1.8. The latter is the Model 3 pulsed compressor planar cascade in Reference [6]. The purpose of this calculation is to explore the feasibility of using the mean stream method on an axial flow compressor planar cascade. References [4] and [6] only gave the experimental data of the above two cascades at low velocities. Therefore, in our calculation we assumed that the working medium is an incompressible fluid.

From Figures 14 and 15, it can be found that the calculated results are in satisfactory agreement with the experimental data (the results of turbine cascades are even better. For compressor cascade, although the absolute values of the velocity distribution are slightly different, yet more importantly the trend of velocity distribution variation is completely consistent). It completely satisfies the requirement of engineering calculation. In addition, in the calculation we have verified that the use of the analytical method to solve the forward problem is effective and fast. For both types of cascades, it only requires about five trial runs to fit all the coordinates of the calculation points on the surface of the blade profile. Since it only requires very small amount of time to complete one run, therefore the total required time is not too much.

In the example presented in Section V for the reverse problem, when the mean stream line is a circle and its velocity distribution is a constant, the flow inside the duct is a free

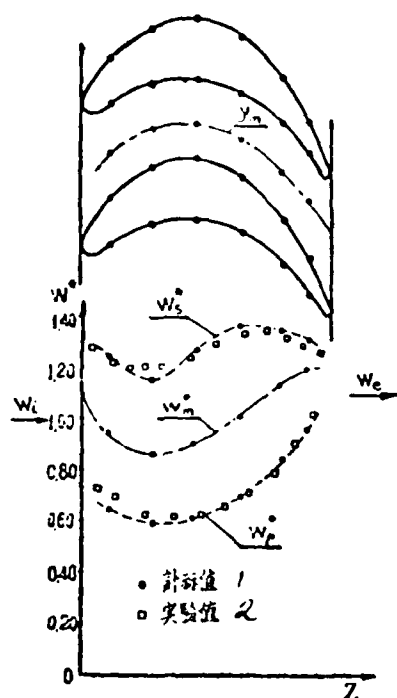


Figure 14. Comparison of Computational Example of the Forward Problem with Experimental Data.  
Key: 1. calculated value, 2. experimental value.

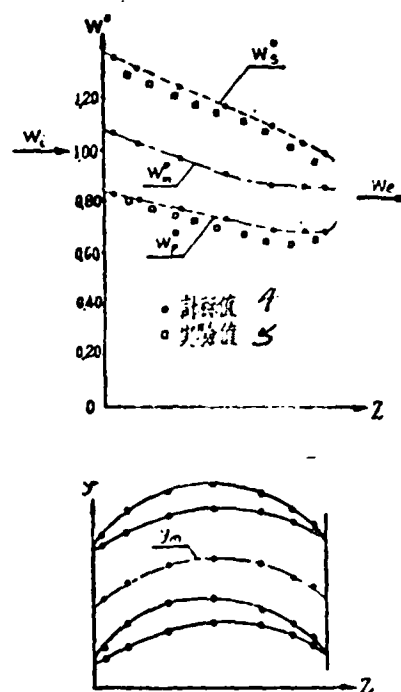


Figure 15. Comparison of Computational Example of the Forward Problem with Experimental Data.  
Key: 4. calculated value, 5. experimental value.

whirlpool. The solution at this time can be obtained rigorously: The boundary of the duct and the mean stream line are concentric circles and the velocity distributions on them are also constants. Their specific numerical values can also be easily obtained. Comparing the results of the rigorous solution and those obtained using the method mentioned in this paper, we can see that they are completely consistent. There is only very small difference in a small segment of the front and rear fringes and those areas are not supposed to be accurately determined by the mean stream line method. This also demonstrated the accuracy of this method.

Finally, it should be pointed out that: the above calculations in the examples although were carried out using ordinary slide rules yet the coordinate points on the surface of the blade profile are very smooth (when slight unsmoothness is found in a certain location, it can even be used as an indication that there is a problem in calculation at this point and requires an examination). From this the advantage of the analytical method is fully demonstrated (There is some slight scatter of the coordinates obtained using the numerical solution. Refer to Reference [3]).

#### IX. Conclusions and Projections

This paper presented an improvement procedure for the mean stream line method - using the analytical solution. This improvement can significantly simplify and speed up the calculation process. It does not require the multiple usage of numerical differentiations. Slide rules can be used in the calculation. The work load required to correct a mistaken term is also very small. It also simultaneously raises the accuracy drastically. In addition, we can control the design variables to calculate good blade profiles. Therefore, this method should be recommended in the design and calculation of turbine cascades of usual densities and pulsed compressor cascades of high densities.

Other than that, the analytical solution itself still has a lot of room for further development which is yet to be explored. For example, using its high calculation speed characteristic, we can obtain a series of cascades for comparison to provide detailed information on the selection of parameters in the design of cascades or to even directly obtain a family of cascades to be selected for use. Because the analytical solution is used, it also opened the possibility of using direct analytical method (even in approximations) to

determine the optimal design parameters. When it is necessary, the analytical solution also allows the conditions that higher terms of the Taylor series expansion with respect to the y-direction must be used. This is because that first higher order derivatives can be more precisely determined (it is not easy to obtain accurate values using numerical differentiations) and secondly the use of more terms of the Taylor series will not be complicated by too much as compared to the use of the numerical solution. Thus further expansion of the Taylor series in the y-direction can be used. Then it is possible to design general compressor cascades and to select the inner (outer) arc of the turbine cascades to calculate the outer (inner) arc using the mean stream line method. Especially, it is highly probably to design axial compressor cascades with higher density near the inner radius using this method. Figure 15 is a preliminary example of such a case. Although the density of a conventional cascade is much less dense, yet its curvature is also much smaller. This corresponds to the use of a small segment in the z direction of the blade profile as the expansion region for the calculation. Therefore, it seems that it is even possible to use only the first three terms of the Taylor series to calculate compressor cascades. The capability of designing one blade surface from the surface of one blade profile of the turbine cascade also provides advantageous conditions to assure its technological and aerodynamic properties. In addition, it is also worth considering as to how the problems on the arbitrary revolving surfaces and binary ducts (such as the axi-symmetrical gas inlet tube and the compressor tube of turbine cascades) can be solved using the results of the analytical solution. For all these, we wish that development will be gradually make in the future.

Under the guidance of the authors and Comrade Chiang Shih Yen, students of the 1963 class of Tsing Hua University



gas combustion machinery group, Liu Chin Yu, Shu Weu Tao, Show Shau Hau, Wang Chan, Kuo Kao Tsian and Chen Chun Hua have explored part of the problems discussed in this paper in their graduation designs to various extents. Professor Wu Chun Hua has reviewed this paper in detail and often offered valuable suggestions on the developmental direction and problems in this work. Comrade Zhang Chu Chow has plotted all the figures on this paper. We wish to express thanks to all of them.

#### References

- [1] Wu Chung-hua, Brown C. A.; "A Theory of the Direct Inverse Problems of Compressible Flow Past Cascade of Arbitrary Airfoils" J.A.S.; Vol. 19; No. 3; 1952.
- [2] Wu Chun Hua "The Method to Solve Compressible Gas Flow Through Cascades on an Arbitrary Revolving Surface and the Design of Such Cascades" Journal of Mechanical Engineering, 4, Vol. 1, 1956.
- [3] Liu Kao Len, Shih Ming Lum and Wu Chun Hua, "Design and Analysis of the Aerodynamic Turbine Machinery", Journal of Mechanical Engineering, 1, Vol. 1, 1963.
- [4] Dunavant J.C., Erwin J.R.: "Investigation of a Related Series of Turbine-Blade Profiles in Cascade" NACA TN3802; 1956.
- [5] [5] Жуковский М. Н.: "Расчет обтекания решеток профилей турбомашин"; Машгиз; 1960.
- [6] Erwin J.R., Schulze W.M.: "Investigation of an Impulse Axial-flow Compressor"; NACA RM L9J05a; 1950.
- [7] Lin Kao Len "Aerodynamics of Turbine Machinery", Chinese Science and Technical University, 1964.

#### APPENDIX

The following two tables are presented in the appendix:

- 1. Table 2. Table of Special Equations when Frequently Used Geometrical Curves are Chosen to be the Mean Stream Line.
- 2. Table 3: Table of Functions and Equations of Functions Used in the Calculation.

Table 2. Table of Special Equations When Frequently Used Curves are Used as the Mean Stream Line.

3	1	2
1	几何曲线 4	圆弧 5
2	解析关系式 6	$y^2 + z^2 = r^2$
3	$\beta =$	$\tan^{-1} \left[ -\frac{z}{y} \right]$
4	$\beta' =$	$-\frac{1}{r} \cdot \frac{1}{\cos \beta}$
5	$\beta'' =$	$\frac{1}{r^2} \cdot \frac{\sin \beta}{\cos^3 \beta}$
6	$\left( \frac{\partial W'}{\partial y} \right)_B =$	$C_1 \cdot \frac{W}{r} + B_1 \cdot W'$
7	$\left( \frac{\partial^2 W'}{\partial y^2} \right)_B =$	$C_2 \cdot \frac{W}{r^2} + C_3 \cdot \frac{W'}{r} + B_2 \cdot W''$
8	$\frac{\partial W}{\partial y} = \left( \frac{\partial W}{\partial y} \right)_B =$	$-\frac{W}{r} \cdot \cos \beta + B_3 \cdot W'$
9	$\left( \frac{\partial^2 W}{\partial y^2} \right)_B =$	$C_4 \cdot \frac{W}{r^2} + C_5 \cdot \frac{W'}{r} + B_{12} \cdot W'' + B_{13} \cdot \frac{W'^2}{W}$
10	$\frac{1}{\rho} \frac{\partial (\rho W'_z)}{\partial y} =$	$\left( \frac{\partial W_z}{\partial y} \right)_B + M^2 \left( B_7 \cdot \frac{W}{r} - B_8 \cdot W' \right)$
11	$\frac{1}{\rho} \frac{\partial^2 (\rho W'_z)}{\partial y^2} =$	$\left( \frac{\partial^2 W_z}{\partial y^2} \right)_B + M^2 \left[ C_6 \cdot \frac{W}{r^2} + C_7 \cdot \frac{W'}{r} + B_{16} W'' + B_{19} \frac{W'^2}{W} \right]$ $+ M^4 \left[ (2 - \gamma) B_{14} \cdot \left( \frac{W}{r^2} \right) - (7 - 3\gamma) B_{10} \cdot \frac{W'}{r} - B_{20} W'' \right]$ $+ (B_{21} - \gamma \cdot B_6) \frac{W'^2}{W'} - M^6 \cdot \gamma \cdot B_{20} \cdot \frac{W'^2}{W}$
12	$\frac{\partial^2 W'}{\partial y^2} =$	$\left( \frac{\partial^2 W'}{\partial y^2} \right)_B + M^2 \left[ \frac{1}{2} B^2 \cdot \frac{W'}{r} + B_{13} \left( W'' + M^2 \cdot \gamma \cdot \frac{W'^2}{W} \right) \right]$

Key: 2. Colume 3. Now; 4. Geometric Curve, 5. Analyticaly relation, 6. Circular arc, 7. Second Order Parabolic Curve.

Table 2 Cont'd.

3
二次拋物線 7
$y = \eta z^2 + 0z + \lambda$
$\tan^{-1}(2\eta z + 0)$
$2\eta \cdot \cos^2 \beta$
$-8\eta^2 \cos^3 \beta \sin \beta$
$P_1(2\eta)W + B_2W'$
$P_2(2\eta)^2 \cdot W + P_3(2\eta)W' + B_6 \cdot W^2$
$B_{13}(2\eta)W + B_8W'$
$P_4 \cdot (2\eta)^2 \cdot W + P_5(2\eta)W' + B_{12} \cdot W^2 + B_{18} \cdot \frac{W'^2}{W}$
$\left(\frac{\partial W_2}{\partial y}\right)_B - M^2[B_{20} \cdot (2\eta) \cdot W + B_2W']$
$\left(\frac{\partial^2 W_2}{\partial y^2}\right)_B + M^2\left[P_7(2\eta)^2W + P_8(2\eta)W' + B_{16}W^2 + B_{19}\frac{W'^2}{W}\right]$ $+ M^4\left[(2-\gamma)P_9(2\eta)^2W + (7-3\gamma) \cdot P_{10}(2\eta)W' - B_{20}W^2\right.$ $\left.+ (B_{21} - \gamma \cdot B_6)\frac{W'^2}{W}\right] - M^6 \cdot \gamma \cdot B_{20} \cdot \frac{W'^2}{W}$
$\left(\frac{\partial^2 W}{\partial y^2}\right)_B + M^2\left[-P_6(2\eta)W' + B_{13}\left(W^2 + M^2 \cdot \gamma \cdot \frac{W'^2}{W}\right)\right]$

Table 2 Cont'd.

1	2	3	4
1			三次拋物線 $\psi$
2			$y = \eta z^3 + \lambda$
3			$\tan^{-1}(3\eta z^2)$
4			$6\eta z \cdot \cos^2 \beta$
5			$6\eta \cos^2 \beta (4 \cos^2 \beta - 3)$
6			$P_1(6\eta) z \cdot W + B_3 W'$
7			$T_1(6\eta) W + P_3(6\eta) z \cdot W' + B_6 W''$
8			$B_{13}(6\eta) z \cdot W + B_8 W''$
9			$T_2(6\eta) W' + P_5(6\eta) z \cdot W' + B_{12} W'' + B_{13} \frac{W'^2}{W}$
10			$\left( \frac{\partial W''}{\partial y} \right)_B - M^2 [B_{20}(6\eta) z \cdot W + B_2 W']$
11			$\left( \frac{\partial^2 W}{\partial y^2} \right)_B \left[ + M^2 [T_3(6\eta) W + P_8(6\eta) z \cdot W' + B_{18} W'' + B_{19} \frac{W'^2}{W}] \right.$ $+ W^4 [ (2 - \gamma) T_4(12\eta) W' + (7 - 3\gamma) P_{10}(6\eta) z \cdot W' - B_{20} W''$ $\left. + (B_{21} - \gamma B_6) \frac{W'^2}{W} ] - M^6 \cdot \gamma \cdot B_{20} \frac{W'^2}{W} \right]$
12			$\left( \frac{\partial^3 W}{\partial y^3} \right)_B + M^2 \left[ -6(6\eta) z \cdot W' + B_{13} \left( W'' + M^2 \cdot \gamma \cdot \frac{W'^2}{W} \right) \right]$

Key: 1. Column, 2. Now, 3. (Continuation), 4. Third Order Parabolic Curve, 5. Equi z - directional angle variation curve.

(12), 3

5

TABLE 5

$$\gamma = \frac{1}{\eta} \ln \sec(\eta^2 + 0) + \lambda$$

$$\eta^2 + 0$$

$$\eta$$

$$0$$

$$H_1 \eta_1 W' + H_2 W''$$

$$H_3 \eta_1^2 W' + H_4 \eta_1 W'' + H_5 W'''$$

$$H_7 \eta_1 W' + H_8 W''$$

$$B_9 \eta_1^2 W' + H_{11} \eta_1 W'' + H_{12} W''' + H_{13} \frac{W''^2}{W'}$$

$$\left( \frac{\partial W'}{\partial y} \right)_n - M^2 (H_{14} \eta_1 W' + H_{15} W'')$$

$$\begin{aligned} & \left( \frac{\partial^2 W'}{\partial y^2} \right)_n + M^2 \left[ H_{17} \eta_1^2 W' + H_{17} \eta_1 W'' + H_{18} W''' + H_{19} \frac{W''^2}{W'} \right] \\ & + M^2 \left[ (2 - \gamma) H_{20} \eta_1^2 W' + (7 - 3\gamma) H_{10} \eta_1 W'' - H_{10} W''' + (H_{21} - \gamma B_9) \frac{W''^2}{W'} \right] \\ & - M^2 \cdot \gamma H_{20} \frac{W''^2}{W'} \end{aligned}$$

$$\left( \frac{\partial^2 W'}{\partial y^2} \right)_n + M^2 \left[ -H_{10} \eta_1 W'' + H_{12} \left( W''^2 + M^2 \cdot \gamma \cdot \frac{W''^2}{W'} \right) \right]$$

Table 2 Cont'd.

3 fi	2	6			
		3	2	1	4
1					
2					$y = \eta \cosh (\theta z) + \lambda$
3					$\tan^{-1}[\eta \theta \sinh (\theta z)]$
4					$\theta^2 (y - \lambda) \cos^2 \beta$
5					$\theta^2 \cos \beta \sin \beta [1 - 2 \cos^2 \beta \cdot \theta^2 (y - \lambda)^2]$
6					$P_1 \theta^2 (y - \lambda) W + B_2 W'$
7					$[\theta^4 (y - \lambda)^2 P_2 + \theta^2 H_1] W + P_3 \theta^2 (y - \lambda) W' + B_6 W''$
8					$H_2 \theta^2 (y - \lambda) W + B_8 W'$
9					$[\theta^4 (y - \lambda)^2 P_4 + \theta^2 H_2] W + P_5 \theta^2 (y - \lambda) W' + B_{12} W'' + B_{13} \frac{W'^2}{W}$
10					$\left( \frac{\partial W}{\partial y} \right)_H - M^2 [B_{20} \theta^2 (y - \lambda) W + B_2 W']$
11					$\left( \frac{\partial^2 W}{\partial y^2} \right)_H + M^2 \left\{ \theta^4 (y - \lambda)^2 P_7 - \theta^2 H_3 \right\} W + \theta^2 (y - \lambda) P_8 W' + B_{18} W''$ $+ B_{19} \frac{W'^2}{W} + M^2 \left[ (2 - \gamma) \theta^4 (y - \lambda)^2 P_9 W + (7 - 3\gamma) \theta^2 (y - \lambda) P_{10} W' \right.$ $\left. - B_{20} W'' + (H_{11} - \gamma H_6) \frac{W'^2}{W} \right] - M^2 \gamma H_{20} \frac{W'^2}{W}$
12					$\left( \frac{\partial^2 W'}{\partial y^2} \right)_H + M^2 \left[ -P_6 \theta^2 (y - \lambda) W' + B_{13} \left( W'' + M^2 \gamma \frac{W'^2}{W} \right) \right]$

Key: 1. Continuation; 2. Column, 3. Row, 4. Suspended Chain Curve, 5. Cosine Curve.

(續) /

7

三角余弦綫 5

$$y = \eta \cos(\theta Z) + \lambda$$

$$\tan^{-1}[-\eta \theta \sin(\theta Z)]$$

$$-\theta^2(y - \lambda) \cos^2 \beta$$

$$-\theta^2 \cos \beta \sin \beta [1 + 2 \cos^2 \beta \theta^2 (y - \lambda)^2]$$

$$-P_1 \theta^2 (y - \lambda) W + B_2 W'$$

$$[\theta^4 (y - \lambda)^2 \cdot P_2 - \theta^2 H_1] W - P_3 \theta^2 (y - \lambda) W' + B_0 W''$$

$$-B_{13} \theta^2 (y - \lambda) W + B_8 W'$$

$$[\theta^4 (y - \lambda)^2 P_4 - \theta^2 H_2] W - P_5 \theta^2 (y - \lambda) W' + B_{12} W'' + B_{13} \frac{W'^2}{W}$$

$$\left( \frac{\partial W_3}{\partial y} \right)_B + M^2 [B_{20} \theta^2 (y - \lambda) W - B_2 W']$$

$$\left( -\frac{\partial W_3}{\partial y^2} \right)_B + M^2 \left\{ [\theta^4 (y - \lambda)^2 P_7 + \theta^2 H_3] W - \theta^2 (y - \lambda) P_8 W' + B_{18} W'' + B_{19} \frac{W'^2}{W} \right\} + M^4 \left[ (2 - \gamma) \theta^4 (y - \lambda)^2 P_9 W - (7 - 3\gamma) \theta^2 (y - \lambda) P_{10} W' - P_{20} W'' + (B_{21} - \gamma B_0) \frac{W'^2}{W} \right] - M^6 \gamma B_{20} \frac{W'^2}{W}$$

$$\left( -\frac{\partial^2 W}{\partial y^2} \right)_B + M^2 \left[ P_6 \theta^2 (y - \lambda) W' + B_{13} \left( W'' + M^2 \cdot \gamma \cdot \frac{W'^2}{W} \right) \right]$$

51

Table 3. Table of Functions Used in the Calculation

表3 計算

函 数	$\cos \beta$	$\sin \beta$	$B_1$	$B_2$	$B_3$	$B_4$	$B_5$
公 式			$\cos \beta (2 \cos^2 \beta - 1)$	$2 \cos^2 \beta \sin \beta$	$\cos \beta (12 \cos^4 \beta - 11 \cos^2 \beta + 1)$	$\cos^2 \beta \sin \beta \times (4 \cos^2 \beta - 1)$	$2 \cos^2 \beta \sin \beta \times (8 \cos^2 \beta - 3)$
函数性质	偶	奇	偶	奇	偶	奇	奇
$\beta = 0^\circ$	1.0000	0.0000	.0000	0.0000	2.0000	0.0000	0.0000
5°	0.9962	0.08716	0.9811	0.1730	1.8947	0.2569	0.8544
10°	0.9848	0.1736	0.9254	0.3368	1.5943	0.4849	1.6029
15°	0.9659	0.2588	0.8365	0.4830	1.1427	0.6597	2.1560
20°	0.9397	0.3420	0.7198	0.6040	0.6047	0.7647	2.4549
25°	0.9063	0.4226	0.5826	0.6943	0.05521	0.7934	2.4794
30°	0.8660	0.5000	0.4330	0.7500	-0.4330	0.7500	2.2500
35°	0.8192	0.5736	0.2802	0.7698	-0.8012	0.6481	1.8228
40°	0.7660	0.6428	0.1330	0.7544	-1.0133	0.5082	1.2784
45°	0.7071	0.7071	0.0000	0.7071	-1.0607	0.3536	0.7071
50°	0.6428	0.7660	-0.1116	0.6330	-0.9618	0.2066	0.1933
55°	0.5736	0.8192	-0.1962	0.5390	-0.7572	0.08515	-0.1984
60°	0.5000	0.8660	-0.2500	0.4330	-0.5000	0.0000	-0.4330
65°	0.4226	0.9063	-0.2717	0.3237	-0.2459	-0.04623	-0.5087
70°	0.3420	0.9397	-0.2620	0.2198	-0.04192	-0.05849	-0.4538
75°	0.2588	0.9659	-0.2241	0.1294	0.08204	-0.04737	-0.3189
80°	0.1736	0.9848	-0.1632	0.05939	0.1179	-0.02611	-0.1638

Key: 2. Function, 3. Equation, 4. Functional Characteristics,  
5. Even, 6. Odd.



用函数表

$B_6$	$B_7$	$B_8$	$B_9$	$B_{10}$	$B_{11}$	$B_{12}$	$B_{13}$
$\cos^3 \beta (3 - 4 \cos^2 \beta)$	$\cos^2 \beta$	$\cos \beta \sin \beta$	$\cos^2 \beta \times (5 \cos^2 \beta - 3)$	$\cos^3 \beta \sin \beta$	$\cos \beta \sin \beta \times (6 \cos^2 \beta - 1)$	$\cos^2 \beta \times (1 - 2 \cos^2 \beta)$	$\cos^4 \beta$
偶 1	偶 2	奇 3	偶 4	奇 5	奇 6	偶 7	偶 8
-1.0000	1.0000	0.0000	2.0000	0.0000	0.0000	-1.0000	1.0000
-0.9586	0.9924	0.08682	1.9471	0.08617	0.4302	-0.9773	0.9849
-0.8399	0.9698	0.1710	1.7935	0.1659	0.8241	-0.9114	0.9406
-0.6597	0.9330	0.2500	1.5535	0.2333	1.1495	-0.8080	0.8705
-0.4415	0.8930	0.3214	1.2496	0.2838	1.3814	-0.6764	0.7797
-0.2126	0.8214	0.3830	0.9093	0.3146	1.5046	-0.5280	0.6747
0.0000	0.7500	0.4330	0.5625	0.3248	1.5155	-0.3750	0.5625
0.1728	0.6710	0.4698	0.2382	0.3137	1.4218	-0.2295	0.4503
0.2934	0.5868	0.4924	-0.03266	0.2890	1.2413	-0.1019	0.3444
0.3536	0.5000	0.5000	-0.2500	0.2500	1.0000	0.0000	0.2500
0.3578	0.4132	0.4924	-0.3860	0.2035	0.7283	0.07175	0.1707
0.3178	0.3290	0.4698	-0.4458	0.1546	0.4576	0.1125	0.1082
0.2500	0.2500	0.4330	-0.4375	0.1083	0.2165	0.1250	0.06250
0.1725	0.1786	0.3830	-0.3763	0.06841	0.02744	0.1148	0.03190
0.1013	0.1170	0.3214	-0.2825	0.03757	-0.09582	0.08961	0.01368
0.04737	0.06699	0.2500	-0.1785	0.01675	-0.1495	0.05801	0.004187
0.01508	0.03015	0.1710	-0.08591	0.005157	-0.1401	0.02834	0.0009092

Key: 1, 2, 4, 7, 8. Even, 3, 5, 6. Odd.

表3 計算用函

圖 2	$B_{14}$	$B_{15}$	$B_{16}$	$B_{17}$	$B_{18}$	$B_{19}$	$B_{20}$
公 式	$\cos^3 \beta$	$\cos^3 \beta \times (5 - 11\cos^2 \beta)$	$\cos^4 \beta \sin \beta$	$\cos^2 \beta \sin \beta \times (6 - 26\cos^2 \beta)$	$\cos^3 \beta \times (5\cos^2 \beta - 3)$	$\cos^3 \beta \times (10\cos^2 \beta - 9)$	$\cos^5 \beta$
函數性質	偶	偶	奇	奇	偶	偶	偶
$\beta = 0^\circ$	1.0000	-5.0000	0.0000	0.0000	2.0000	1.0000	1.0000
5°	0.9386	-4.8605	0.08584	-1.7128	1.9397	0.9135	0.9811
10°	0.9551	-4.4588	0.1633	-3.2362	1.7662	0.6671	0.9263
15°	0.9012	-3.8420	0.2253	-4.4091	1.5006	0.2975	0.8409
20°	0.8298	-3.0812	0.2667	-5.1217	1.1742	-0.1409	0.7327
25°	0.7444	-2.2596	0.2851	-5.3307	0.8241	-0.5852	0.6115
30°	0.6495	-1.4614	0.2813	-5.0625	0.4871	-0.9743	0.4871
35°	0.5470	-0.7555	0.2583	-4.4054	0.1942	-1.2526	0.3670
40°	0.4495	-0.2046	0.2214	-3.4919	-0.02962	-1.4078	0.2638
45°	0.3536	0.1768	0.1768	-2.4749	-0.1768	-1.4142	0.1768
50°	0.2656	0.3864	0.1308	-1.5011	-0.2481	-1.2929	0.1097
55°	0.1887	0.4493	0.08866	-0.6882	-0.2557	-1.0775	0.06208
60°	0.1250	0.4063	0.05413	-0.1083	-0.2188	-0.8125	0.03125
65°	0.07548	0.3046	0.02891	0.2195	-0.1590	-0.5445	0.01348
70°	0.04001	0.1886	0.01286	0.3252	-0.09663	-0.3133	0.004680
75°	0.01734	0.09125	0.004334	0.2755	-0.04621	-0.1444	0.001161
80°	0.005236	0.02968	0.0008954	0.1549	-0.01492	-0.04555	0.0001579

Key: 5. Even, 6. Odd.

表 (一)

$B_{21}$	$C_1$	$C_2$	$C_3$	$C_4$	$C_5$	$C_6$	$C_7$
$\cos^3 \beta \times$ ( $6-7\cos^2 \beta$ )	$1-2\cos^2 \beta$	$2\cos \beta \times$ ( $4\cos^2 \beta-3$ )	$2\cos \beta \sin \beta \times$ ( $3-8\cos^2 \beta$ )	$3\cos^2 \beta-1$	$\sin \beta \times$ ( $1-6\cos^2 \beta$ )	$\cos \beta \times$ ( $3-8\cos^2 \beta$ )	$\cos \beta \sin \beta \times$ ( $26\cos^2 \beta-6$ )
偶 5	偶 5	偶 5	奇 6	偶 5	奇 6	偶 5	奇 6
-1.0000	-1.0000	2.0000	0.0000	2.0000	0.0000	-5.0000	0.0000
-0.9361	-0.9848	1.9319	-0.8577	1.9772	-0.4318	-4.9204	1.7193
-0.7535	-0.9397	1.7321	-1.6276	1.9095	-0.8368	-4.6855	3.2861
-0.4786	-0.8660	1.4142	-2.2321	1.7990	-1.1901	-4.3120	4.5645
-0.1503	-0.7660	1.0000	-2.6124	1.6491	-1.4700	-3.8191	5.4504
0.1863	-0.6428	0.5176	-2.7357	1.4642	-1.6602	-3.2366	5.8818
0.4871	-0.5000	0.0000	-2.5981	1.2500	-1.7500	-2.5981	5.8457
0.7127	-0.3420	-0.5176	-2.2253	1.0130	-1.7357	-1.9398	5.3780
0.8506	-0.1736	-1.0000	-1.6688	0.7605	-1.6204	-1.2981	4.5584
0.8839	0.0000	-1.4142	-1.0000	0.5000	-1.4142	-0.7071	3.5000
0.8254	0.1736	-1.7321	-0.3008	0.2395	-1.1330	-0.1963	2.3353
0.6976	0.3420	-1.9319	0.3459	-0.01303	-0.7978	0.2111	1.1999
0.5313	0.5000	-2.0000	0.8660	-0.2319	-0.4330	0.5000	0.2165
0.3785	0.6428	-1.9319	1.2036	-0.4642	-0.06492	0.6640	-0.5195
0.2073	0.7660	-1.7321	1.3268	-0.6491	0.2802	0.7060	-0.9509
0.09390	0.8660	-1.4142	1.2321	-0.7990	0.5777	0.6378	-1.0646
0.03031	0.9397	-1.0000	0.9436	-0.9095	0.8066	0.4791	-0.3920

Key: 5. Even, 6. Odd.

1 函 数	$P_1$	$P_2$	$P_3$	$P_4$	$P_5$	$P_6$
2 公 式	$\cos^3 \beta \times (2 \cos^2 \beta - 1)$	$\cos^3 \beta (20 \cos^4 \beta - 21 \cos^2 \beta + 3)$	$2 \cos^4 \beta \sin \beta \times (8 \cos^2 \beta - 3)$	$\cos^5 \beta \times (9 \cos^2 \beta - 7)$	$\cos^3 \beta \sin \beta \times (6 \cos^2 \beta - 1)$	$\cos^5 \beta \sin \beta$
3 函数性质	偶 <sup>4</sup>	偶 <sup>4</sup>	奇 <sup>5</sup>	偶 <sup>4</sup>	奇 <sup>5</sup>	奇 <sup>5</sup>
$\beta = 0^\circ$	1.0000	2.0000	0.0000	2.0000	0.0000	0.0000
5°	0.9736	1.8218	0.8479	1.8880	0.4269	0.08551
10°	0.8975	1.3388	1.5545	1.5772	0.7993	0.1609
15°	0.7805	0.6870	2.0116	1.1347	1.0725	0.2176
20°	0.6356	0.03745	2.1677	0.6522	1.2198	0.2506
25°	0.4785	-0.4620	2.0365	0.2400	1.2359	0.2584
30°	0.3248	-0.7307	1.6875	-0.1055	1.1367	0.2436
35°	0.1871	-0.7657	1.2231	-0.2903	0.9204	0.2105
40°	0.07806	-0.6426	0.7502	-0.3473	0.7284	0.1696
45°	0.0000	-0.4419	0.3536	-0.3125	0.5000	0.1250
50°	-0.04612	-0.2483	0.07988	-0.2315	0.3009	0.08406
55°	-0.06454	-0.1083	-0.06527	-0.1438	0.1505	0.05085
60°	-0.06250	-0.03125	-0.1083	-0.07422	0.05413	0.02706
65°	-0.04852	-0.001520	-0.09085	-0.03072	0.004901	0.01222
70°	-0.03065	0.003824	-0.05309	-0.009520	-0.01120	0.004398
75°	-0.01502	0.001955	-0.02136	-0.001923	-0.01002	0.001218
80°	-0.004920	0.0003766	-0.004961	-0.0001845	-0.004224	0.0001555

Key: 1. Function, 2. Equation, 3. Functional Characteristics,  
4. Even, 5. Odd.

$P_7$	$P_8$	$P_9$	$P_{10}$	$T_1$	$T_2$
$\cos^7 \beta \times$ (12-17cos <sup>2</sup> β)	$\cos^4 \beta \sin \beta \times$ (6-26cos <sup>2</sup> β)	$\cos^3 \beta$	$\cos^6 \beta \sin \beta$	$\cos^4 \beta \sin \beta (40\cos^4 \beta$ $-38\cos^2 \beta + 5)$	$6 \cos^5 \beta \sin \beta \times$ (3 cos <sup>2</sup> β - 2)
偶 <sup>4</sup>	奇 <sup>5</sup>	偶 <sup>4</sup>	奇 <sup>5</sup>	奇 <sup>5</sup>	奇 <sup>5</sup>
-5.0000	0.0000	1.0000	0.0000	0.0000	0.0000
-4.7426	-1.6938	0.9663	0.08519	-0.5737	0.5014
-4.0314	-3.1386	0.8713	0.1584	0.9424	0.8778
-3.0292	-4.1137	0.7320	0.2102	0.9837	1.0434
-1.9484	-4.5226	0.5713	0.2355	0.7025	0.9759
-0.9863	-4.3786	0.4126	0.2342	0.2209	0.7197
-0.2740	-3.7969	0.2740	0.2109	-0.2813	0.3654
0.1460	-2.9561	0.1653	0.1733	-0.6426	0.01646
0.3133	-2.0491	0.09084	0.1299	-0.7802	-0.2437
0.3094	-1.2374	0.04419	0.08839	-0.7071	-0.3750
0.2256	-0.6202	0.01873	0.03403	-0.5064	-0.3836
-0.1309	-0.2264	0.006719	0.02917	-0.2813	-0.3091
-0.06055	-0.02706	0.001953	0.01353	-0.1083	-0.2030
0.02159	0.03921	0.0003301	0.005164	-0.01477	-0.1073
0.005481	0.03804	0.00006404	0.001504	0.01417	-0.04351
0.0008450	0.01846	0.000005212	0.0002904	0.01142	-0.01211
0.00005469	0.004671	0.0000001436	0.00002700	0.003494	-0.001782

Table 3. Table of Functions Used in the Calculations (concentration 3)

function	$T_0$	$T_1$	$H_1$	$H_2$	$H_3$
equation	$\cos^4 \beta \sin \beta \times$ (21 - 34 $\cos^2 \beta$ )	$\cos^4 \beta \sin \beta$	$\cos^3 \beta \sin^2 \beta \times$ (4 $\cos^2 \beta - 1$ )	$2 \cos^4 \beta \sin^2 \beta$	$3 \cos^5 \beta \sin^2 \beta$
functional characteristics	odd	odd	even	even	even
$\beta = 0^\circ$	0.0000	0.0000	0.0000	0.0000	0.0000
5°	-1.0854	0.08454	0.02230	0.01496	0.02236
10°	-1.8969	0.1536	0.08293	0.05673	0.08380
15°	-2.2540	0.1961	0.1649	0.1166	0.1690
20°	-2.1248	0.2079	0.2458	0.1824	0.2571
25°	-1.6225	0.1904	0.3039	0.2410	0.3276
30°	-0.9492	0.1582	0.3248	0.2813	0.3654
35°	-0.2237	0.1163	0.3045	0.2963	0.3623
40°	0.1361	0.07623	0.2502	0.2846	0.3270
45°	0.3536	0.04416	0.1768	0.2500	0.2652
50°	0.3756	0.02232	0.1017	0.2004	0.1932
55°	0.2863	0.009596	0.04001	0.1453	0.1250
60°	0.1692	0.003383	0.0000	0.09375	0.07031
65°	0.07708	0.0009223	-0.01771	0.05241	0.03322
70°	0.02561	0.0001760	-0.01880	0.02417	0.01240
75°	0.005436	0.00001945	-0.01184	0.008373	0.003251
80°	0.0005393	0.0000008142	-0.00466	0.001764	0.0004594

THE ANALYTICAL SOLUTION OF MEAN-STREAM LINE  
METHOD FOR TWO-DIMENSIONAL CASCADES  
—SOME DEVELOPMENT OF MEAN-  
STREAM LINE METHOD(I)—

Tsay Ruey-shen

ABSTRACT

A modification of mean-stream line method is presented. With this modification, an computation of two-dimensional cascade can be calculated analytically and the accuracy solution is higher than the original method as well as the time needed for one complete calculation is shorter. Some examples of solution are compared and discussed for finding the better form of the mean-stream line and the better variation of velocity along the mean-stream line. With this discussion and the equations and tables presented in this paper, only about 8 hours are needed for projecting a good turbine cascade circulated by compressible flow, and the iteration in the direct problem to fit the given blade shape is more practical. The results of calculation of this method compared well with experimental data. Some probabilities of development of the mean-stream line method are discussed in the end of this paper.

# CALCULATION OF TRANSONIC FLOW IN PLANAR CASCADES - SOME DEVELOPMENT OF MEAN STREAM LINE METHOD (IV)

Tsay Ruey-shen

## Abstract

Because the equations of the mean stream line method are consistent at subsonic and supersonic speed and there does not exist an odd point at  $M=1$ , therefore they can be used to calculate transonic flow in the cascades. Comparing the calculated results with the experimental data, we found that it is feasible to use this method. The approximate range of conditions under which this method is applicable is also analysed in this paper.

## Symbols

a	sonic speed
B	function of $\beta$ <sup>[3]</sup>
l	coordinate in the direction of the stream line
M	Mach number of the gas flow
n	direction normal to that of the stream line
$\Delta n$	distance of expansion in the n direction
q	$\rho_w / \rho_w$ relative flow density of the gas flow
W	velocity of the gas flow
y	coordinate tangent to the direction of the cascade
$\Delta y$	distance of expansion in the y direction
z	axial coordinate of the turbine machinery
$\beta$	arc tg $(\frac{dy}{dz})$ , gas flow angle
$\gamma$	ratio of specific heats of gases
$\lambda$	$W/a$ , relative velocity of the gas flow
$\rho$	density of the gas
$\psi$	flow function
$\Delta \psi$	amount of flow within the distance of expansion



$\Omega$  radius of curvature of the stream line

#### Superscript

$d/dz$ , total differentiation with respect to the  $z$  direction

#### Subscript

$l$  component in the  $l$  direction  
 $m$  value on the mean stream line (selected)  
 $p$  value on the inner arc of the blade profile  
 $s$  value on the back arc of the blade profile  
 $z$  component in the  $z$  direction  
 $l$  value under one-dimensional assumption  
 $1.2---n$  different functions  
 $*$  critical values of the gas flow

### I. Introduction

In recent years transonic cascades have been widely used in turbine machinery, it is there imperative to obtain better understanding about the state of flow in those cascades. It is well known that even under the simplified condition of an ideal gas flow in a planar cascade, there is a certain degree of mathematical difficulty in solving for the transonic flow. This is because that the basic differential equations describing the flow in the subsonic and supersonic regions are different types. One is the elliptical type while the other is the hyperbolic type. It is not convenient to treat them in an unified manner.

But the above problem only appears in multi-dimensional equations. In one-dimensional flow, the subsonic and supersonic flows are both represented by an integrated algebraic equation with the exception that we must notice that the  $M$

number is a double value function of the flow density. Therefore, we can assume the following: The difficulty in solving the transonic flow problem is because the multi-dimensional flow equation is used directly. If we can initiate the general potential flow theory<sup>[1]</sup> of turbine machinery to continuously decrease the dimensions all the way to one then we can use the simple method to directly obtain the solution of transonic flow. The mean stream line method<sup>[2]</sup> is such a method in nature. It transforms the two-dimensional flow into a flow on the one dimensional flow on the mean stream line  $y_m - y_m(z)$  and the expansion of a flow parameter in another direction (usually in the tangential direction  $y$  of the turbomachine. Thus it may be possible to solve the transonic flow problem using an unified mathematical treatment. Especially if the analytical solution method is used instead of the numerical method, it is much more easier to verify this possibility and more suitable for the kind of calculation accuracy required in the transonic region.

Based on the above consideration, this paper presents a discussion of solving the transonic flow in planar cascades using the mean stream line method. Detailed introduction of this method has already been documented in References [2] and [3], so it is not repeated here.

## II. Equations of Mean Stream Line Method Applicable to Transonic Flow

Reference [3] has derived the equations of the mean stream line method which are suitable for the analytical solution. But in order to be applicable to high speed flow, it is better to alter the forms slightly. In addition, in order to define the boundary of the flow, we still must solve a third order algebraic equation. Finally, we can use the flow

function concept to derive a form which is even easier to solve (see Appendix A). It is summarized in the following:

The partial derivative expanded in the direction tangent to the mean stream line:

$$\left(\frac{1}{\lambda} \frac{\partial^2 \psi}{\partial \eta^2}\right)_m = \left[ B_0 \eta^2 + B_1 \eta + B_2 \left( \frac{\lambda}{\lambda_m} \right) \right]_{\eta=0} \quad (1)$$

$$\begin{aligned} \left(\frac{1}{\lambda} \frac{\partial^3 \psi}{\partial \eta^3}\right)_m = & \left\{ B_0 \eta^3 + 3 B_1 \eta^2 + 3 B_2 \frac{\lambda}{\lambda_m} \eta + B_3 \left( \frac{\lambda}{\lambda_m} \right)^2 \right\}_{\eta=0} \\ & + \lambda_m \left[ (1-B_0) B_0 \eta^2 + (7-3B_0) B_1 \eta + (3-7B_0) B_2 \left( \frac{\lambda}{\lambda_m} \right) \right]_{\eta=0} \quad (2) \end{aligned}$$

$$\left(\frac{1}{\lambda} \frac{\partial^4 \psi}{\partial \eta^4}\right)_m = (C_0 \eta^4 + C_1 \eta^3)_{\eta=0} \quad (3)$$

$$\left(\frac{1}{\lambda} \frac{\partial^5 \psi}{\partial \eta^5}\right)_m = (D_0 \eta^5 + D_1 \eta^4 + D_2 \eta^3 + D_3 \eta^2 + D_4 \eta + D_5 \left( \frac{\lambda}{\lambda_m} \right)^2)_{\eta=0} \quad (4)$$

The equation which determines the flow boundary is (notice that  $\Delta\psi$  has plus and minus signs):

$$\Delta\psi = \frac{\lambda_m^2}{2} \left[ \frac{1}{\lambda} \frac{\partial^2 \psi}{\partial \eta^2} \right]_{\eta=0} + \frac{1}{6} \left[ \frac{1}{\lambda} \frac{\partial^3 \psi}{\partial \eta^3} \right]_{\eta=0} \left( \frac{\lambda}{\lambda_m} \right)^2 + \dots \quad (5)$$

The equation which determines the velocity distribution is

$$\lambda = \lambda_m \left[ 1 + \left( \frac{1}{\lambda} \frac{\partial^2 \psi}{\partial \eta^2} \right)_m \frac{\eta^2}{2} + \left( \frac{1}{\lambda} \frac{\partial^3 \psi}{\partial \eta^3} \right)_m \frac{\eta^3}{6} + \dots \right] \quad (6)$$

In the practical calculation, usually the remaining small terms in equations (5) and (6) are neglected. The  $B_n$ 's in equations (1) - (4) are simple functions of  $\beta$  and their definitions and numerical values can be found in Reference [3] or in Appendix B. Furthermore,  $\beta'_m$  and  $\beta''_m$  can be obtained from  $W_m(z)$  as:

### III. The Feasibility of Solving Transonic Flow Without Intense Shock Wave Using the Mean Stream Line Method

As discussed above, the mean stream line method reduces a two dimensional planar problem to a one dimensional flow on the mean stream line and the expansion of a flow parameter in another direction. There is not difficulty and doubt in calculating the one dimensional transonic flow. Therefore, the only thing which we must check in solving for the transonic flow is that whether it is feasible to expand into a Taylor series in another direction which intersects the stream line.

Apparently, if at places where there is obvious jumping variations in the flow parameters it is impossible to obtain the solution using the Taylor series expansion. Therefore, the mean stream line method cannot be used in regions with strong shock waves. Besides this point, because the same type of basic equations are used in both the subsonic and supersonic regions in the derivation of these partial differential equations used in the expansion, the equations obtained have no odd point at  $M = 1$ , as long as the flow field varies relatively uniformly and smoothly, it is as effective for subsonic flow as for supersonic flow when using the series expansion method to determine the corresponding flow. Since it is possible to use the mean stream line method for the form, the same method should also be applicable to the latter. For good cascades the flow inside basically varies relatively uniformly and smoothly which coincides with the above requirement. The exceptions are areas near the front and rear stationary points where the mean stream line method cannot be used to obtain accurate solutions.

In addition, we may consider the following: The potential flow is a reversible flow and the boundary condition of planar cascades is usually that homogeneous flow exists at infinite distance both upstream and downstream. Therefore, when it is reduced to a one-dimensional problem, the relation between each flow parameters in the direction of the expansion is also a one-dimensional flow relation (passing through one stream line to infinity and then flowing back on another stream line). There is no difficulty involved such as the ones encountered in the treatment of multi-dimensional transonic problems. The only thing is that the flow variables (there is only one variable in the one dimensional isentropic flow) are not defined through the use of variations of parameters in the direction of the mean stream line.

In the one-dimensional flow, the only difference between the supersonic flow and the subsonic flow is that the flow density of the former is a decreasing function of  $M$  number and latter is an increasing function. When  $M = 1$ ,  $q = 1$  reaches the maximum. Therefore, in the expansion to obtain the solution, it is only natural to consider that these relations should be checked to see whether they are satisfied. In practice, when  $M = 1$ , we should get  $\frac{\partial \rho}{\partial n} = 0$  and  $\frac{\partial^2 \rho}{\partial n^2} \leq 0$ . When  $M < 1$ ,  $\frac{\partial \rho}{\partial n}$  should have the same sign as  $\frac{\partial^2 \rho}{\partial n^2}$ . When  $M > 1$ , they should have opposite signs. Using equations (A - 10) - (A - 12) in Appendix, we can see that these relations are all satisfied.

There was a successful example<sup>[4]</sup> using series expansion in a direction which intersects the stream line to solve for the transonic straight axial nozzle which indicates that the above idea is feasible.

Of course, there is another problem. In the classical

subsonic mean stream line method it is only necessary to use up to second order partial derivative of velocity in the Taylor series expansion. Is it enough to use up to the second order term in the transonic region? In other words, when only up to the second order derivatives are used, how far can the expansion distance be? Can this be applicable to general transonic cascades? This problem will be examined through the actual calculation and qualitative analysis presented in the next section.

#### IV. Expansion Terms and Effective Expansion Distance

The mean stream line method is a simple method which enables us to obtain results in short period of time using slide rules. Therefore, although in principle the more terms we use the more accurate it is, yet in the actual application in subsonic cascades we only used up to the second order partial derivatives of velocity. Of course, we wish that we can do the same thing for the transonic flow. The calculated results indicate that it is possible for ordinary cascades. The examples of the calculation process are shown in Figures 1 and 2. Figure 1 is the NACA turbine cascade whose experiment results are obtained from Figure 42(b) in Reference [5]. In Reference [6], it has carried out a calculation for this cascade using a time related method. The results are also plotted here. From this figure, it can be found that the hand calculation obtained using the mean stream line method is satisfactory. It seems to be even better than the results obtained using the time related method by an electronic computer for this specific example. Figure 2 shows the calculated result for the TP-1A turbine cascade of  $M_{\infty}$  which is also satisfactory.

But trial calculation indicates that, when the  $M_m$  number in actual working condition is larger and  $\lambda'_m$  is also larger,

it is not good to use only up to the second order derivatives of velocity. Or, in other words, it indicates that its effective expansion distance is smaller at this time. This phenomenon can be explained by the nature of the mean stream line method and the expansion equations (Equations (A-12) - (A-15) in the Appendix) in the normal direction of its velocity. Because this method is the simplification of a two-dimensional flow to a one-dimensional flow in the direction of the mean stream line plus the correction in another direction (which is reflected by the partial derivative of the velocity in that direction). Therefore, the more the flow approaches a one-

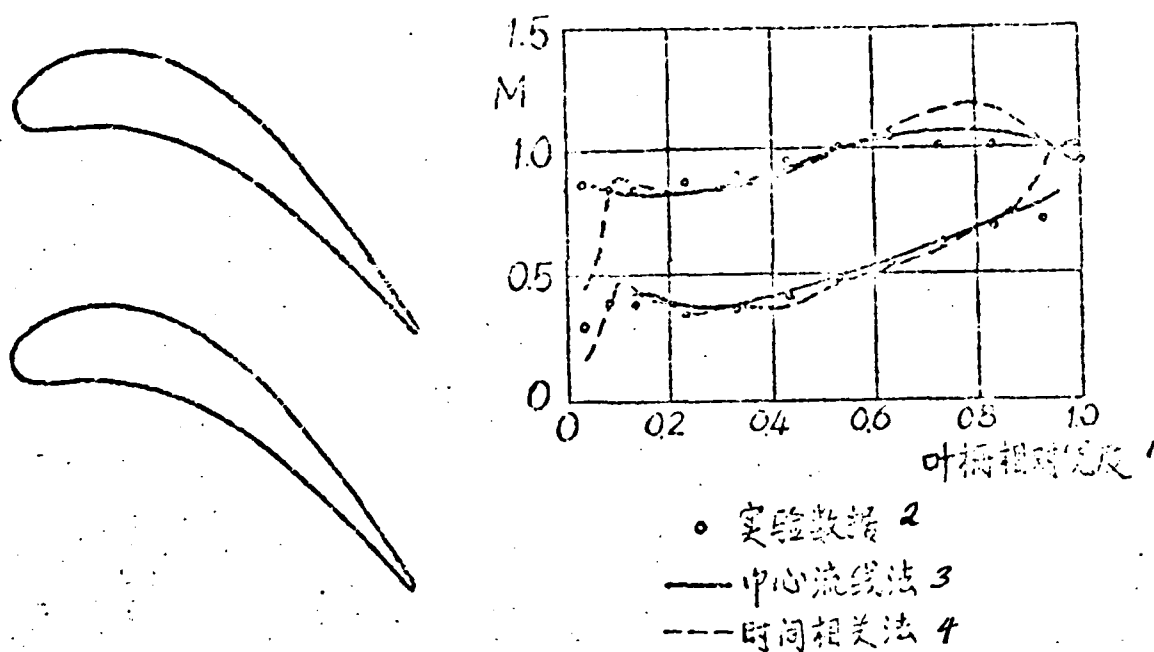


Figure 1. The cascade pattern and its experimental and calculated results. Key: 1. relative width of the cascade, 2. experimental data, 3. mean stream line method, 4. time related method.

dimensional flow or the smaller the value of the partial derivative (the less correction required), the more accurate it is; which also means the farther the allowable expansion distance is. Of course, when the flow curvature  $\frac{1}{R_n}$  with

respect to the width of the flow boundary (corresponding to the width of expansion) and the expansion and contraction of the flow boundary (corresponding to  $(\frac{\partial \lambda}{\partial x})$ ) are smaller, the

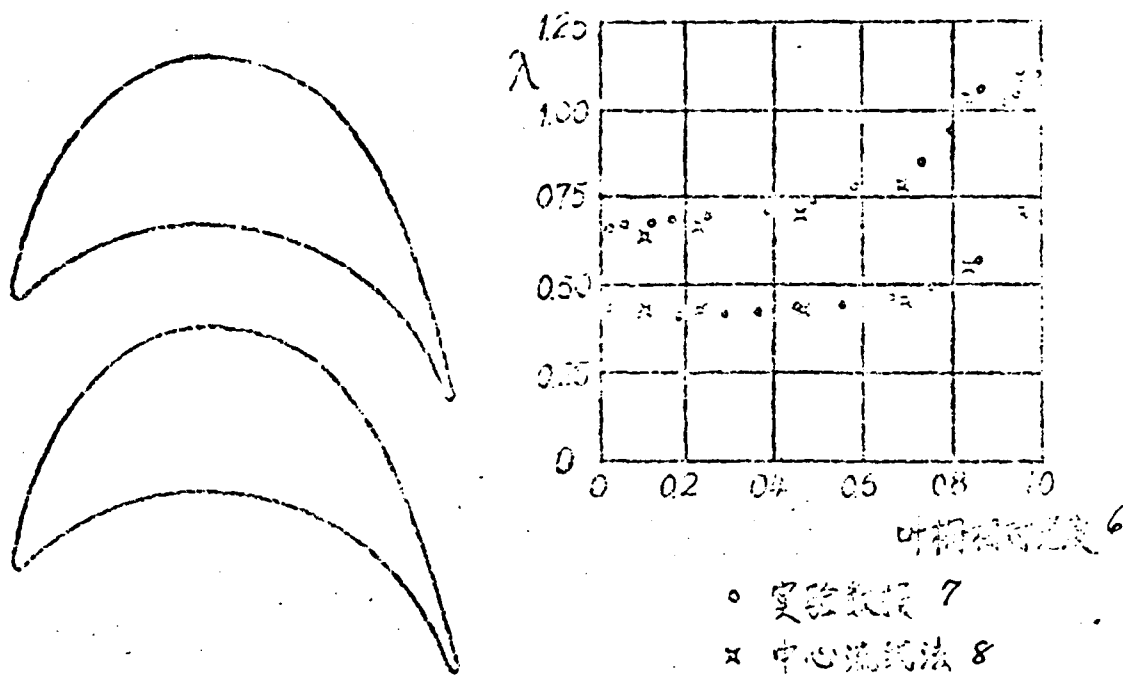


Figure 2. Cascade pattern and its experimental and calculated results. Key: 6. relative width of the cascade, 7. experimental data, 8. mean stream line method.

more close to one-dimensional the flow becomes. Therefore, the application of the mean stream line method should be limited to the situation that  $\frac{\Delta \eta}{\Delta x_m}$  (or  $\frac{\Delta y}{\Delta x_m}$ ) and

$\frac{1}{\lambda} \frac{d\lambda}{dx_m} \Delta \eta$  (or  $(\frac{\lambda}{\Delta x_m} \Delta y)$ ) cannot be too large. This point is also shown in the expansion equations (A-12) - (A-15) because the velocity correction due to the presence of some partial derivatives consists of terms with  $\frac{\Delta \eta}{\Delta x_m}$  and  $(\frac{1}{\lambda} \frac{d\lambda}{dx_m}) \Delta \eta$  (the flow parameter variations of a good cascade is smooth so that only lower order derivatives are considered. From the expression of the first order derivative (A-12), it can



found that it is necessary to require that the term  $\frac{\Delta V}{\Omega_m}$  which is affecting the curvature cannot be too large. If we use this method to obtain the solution of a free whirlpool with variation of direction but no variation in speed and compare the result with the rigorous resolution, we realize that in order to obtain the necessary engineering accuracy usually it is desired to have  $\frac{\Delta V}{\Omega_m} \leq 0.35$  or  $\frac{\Delta \theta}{\Omega_m} \leq 0.35$  (the ordinary good cascades are all within this range). There is another point worthwhile our attention which is that the limitation in the magnitude of  $\frac{\Delta V}{\Omega_m}$  is not related to the Mm number of the flow (see Equations (A-12) and (A-13)). Indeed, the velocity distribution of a free whirlpool is not related to the M number. Therefore, when we use the mean stream line method to solve the free whirlpool or a flow which principally involves a change of direction (corresponding impulsive cascades), Mm has no significant effect on the accuracy of the calculation which means that there is no added difficulty in solving for the transonic flow. However, on the contrary, from equation (A-13) it can be found that the effect of the acceleration  $\frac{dV}{dt}$  on the mean stream line on the accuracy of the calculation is closely related to Mm and it is proportional to  $\frac{1}{Mm}$ . This explains the above phenomenon that when  $\frac{dV}{dt}$  is large if Mm is also large then the effect expansion distance is short. Comparing to the limiting number of  $\frac{dV}{dt}$  for the condition that only turning but no acceleration occurs, if we consider that the same magnitude of limiting number should be applied to the second order partial derivative for the condition that only acceleration but no turning occurs, then approximately we get,  $\frac{dV}{dt} \leq \frac{0.35}{Mm} \Omega_m$  or  $\frac{dV}{dt} \leq 0.35 \sqrt{\frac{\Omega_m}{Mm}}$ . Otherwise the calculated  $\lambda_s$  and  $\lambda_p$  will be too large. Of course, if it turns as well as accelerates, then both limiting regions will have to be even more narrow.

However, it is not a linear additive relationship. Using the Prandtl-Meyer flow with a known rigorous solution to verify this point, we found that this rule is still feasible. The relation between  $M_{eff}$  and  $M$  is shown in Figure 3 (the figure shows the condition under which  $\gamma = 1.4$  and for the generally used  $\gamma$  value the variation of this curve is very small). It can be seen that for the same  $M$ , the effective expansion distance when  $M_m = 1.2$  is only half of that for the incompressible case (under the pure acceleration and no turning condition). Therefore, for supersonic flow, if the acceleration (deceleration) of the gas flow is severe then the use of only up to the second order derivatives in the mean stream line method is not acceptable. But, for an ordinary good cascade (at least for a turbine cascade) the acceleration (deceleration) in the transonic section is relatively slow in order to obtain the good characteristics. Therefore, it is not hindering the use of the mean stream line method which only uses up to the second order derivatives in the calculation. Figure 1 and 2 shown before are such examples.

The above only analyzed the effect of the curvature and acceleration on the mean stream line on the partial derivatives of velocity. The effect on the partial derivatives of the flow density is not mentioned. This is because the two are actually consistent through the equation of the one-dimensional flow. The latter is more complicated to analyze. Since the one-dimensional isentropic flow only has one independent variable, therefore it is sufficient to analyze the derivatives of velocity alone. In addition, the above analysis was mainly carried out using physical diagrams. Mathematically it is better to determine its error or convergence after the derivation of higher order terms of the series. But it is very complicated and may not be necessary for an engineering calculation method such as the mean stream line method.

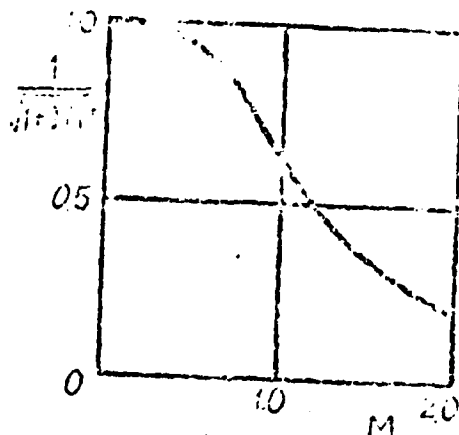
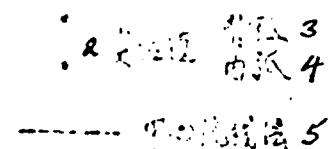



Figure 3. The  $\frac{1}{1+M^2} \sim M$  curve ( $\gamma=1.4$ ).

From the above analysis, we can explain the following facts:

1. The mean stream line method is more suitable for impulsive turbine cascade than for the reversed type [3], [9]. This is because that the latter, with exception of the possibility of having a larger  $\frac{\gamma}{\Omega_m}$ , definitely has a  $(\frac{\gamma}{\Omega_m})_m$  which is much larger than that of the former. Therefore, it corresponds to the fact that the latter has one more factor affecting the inaccuracy of the latter than that of the former.

2. Sometimes (such as the reversed type cascades) the 60% stream line is used as the stream line selected for expansion on both sides which is more effective than choosing the mean stream line [9]. This is because the former sometimes is even closer to the geometric center of the flow boundaries than the latter which makes the expansion distance  $\Delta y$  on either side smaller. Therefore, the expansion is even more accurate.



As an example purposely designed to test the method, Figure 4 shows the calculated results of a supersonic compressor cascade (actually in the experiment acceleration

existed within the flow boundaries). The experimental results are obtained from Reference [10]. Although this cascade has been operating at  $M_m = 1.6 \sim 2.1$ , yet the calculated results (especially in the front half of the flow boundary) still have a certain extent of reliability. In the latter half of the flow boundary  $M$  number has reached above 2.0. Therefore, the  $\lambda_s$  and  $\lambda_p$  obtained from the calculation are both on the high side. From this we can see that the use of the mean stream line method to calculate ordinary transonic cascades ( $M \leq 1.3 \sim 1.4$ ) should be feasible.

Therefore, the presently available relatively simple mean stream line method can be directly extended to the transonic planar cascades. Since the nature and the equations of this method are not changed, all its advantages and disadvantages still remain the same<sup>[2], [3]</sup>. They will not be repeated here. As for the design experience and technique, it is also not difficult to extrapolate from the experience acquired in the subsonic situation as long as the characteristics such as  $q(M)$  has a maximum at  $M = 1$  are noticed. For example in the selection of the position of the mean stream line in the forward problem, in the pure supersonic region it should be chosen closer to the inner arc than the geometric center line which is opposite to that in the subsonic condition.

In order to further increase the accuracy of this method, it is possible to add higher order derivatives as the correction. But the calculation equation will become much more complicated. It also may not be able to expand very far. It may not even be better than the situation that a shorter expansion distance is first chosen in the selection of the stream line expansion to obtain a new stream line and then gradually expand towards the outside to be more effective. However, such a method does not allow the use of the advantages of the mean stream line method<sup>[3]</sup>. Another possible way to solve the high  $M$  flow

problem is to use the mean stream line method to solve the transonic region. After reaching the pure supersonic region, we will change to the uncomplicated supersonic characteristic line method to go on calculating. The total calculation would not be too complicated either.

## V. Conclusions and Projections

Through qualitative analysis and actual calculation, this paper proved that the existing mean stream line method (especially the analytical solution which eliminates the error in numerical differentiation) can be used to calculate flow in an ordinary transonic planar cascade and still maintains the unique characteristics of this method<sup>[2], [3]</sup>. For example, results with sufficient accuracy can be obtained using a slide rule within a couple of days (in the reverse problem). This paper also discussed the limitations of this method.

The extension of the method introduced in this paper to the flow in a cascade on a revolving surface should also be feasible as indicated by the precedent<sup>[11], [12]</sup>.

In addition, as for whether there is a more generalized meaning in the reduction of a multi-dimensional flow problem to an one-dimensional one followed by the use of the characteristic that the one-dimensional flow equation does not have too much difficulty in the transonic region to calculate the flow on a chosen stream line then to expand outward and finally to obtain the transonic flow solution is yet to be studied.

\*Fan Yee-Chien of Nanking Turbine Electric Machinery Factory and L.S. Dzung of BBC in Switzerland have worked in this area.

## References

- [1] Wu Chun-Hua, "A General Theory of Three-Dimensional Flow in Subsonic and Supersonic Turbomachines of Axial, Radial, and Mixed Flow Types"; Trans. ASME, Vol. 74, No. 8; 1952.
- [2] Wu Chun Hua, Brown C.A.: "A Theory of the Direct and Inverse Problems of Compressible Flow Past Cascade of Arbitrary Airfoils," JAS, Vol. 19, No. 3; 1952.
- [3] Tsay Ruey-shen "Analytical Solution of Planar Cascades Using the Mean Stream Line Method - Some Development in the Mean Stream Line Method (I)", Journal of Mechanical Engineering, 14, Vol. 1, 1966.
- [4] Oswatotsck, K., Rothstein, W.: "Flow Pattern in a Converging-Diverging Nozzle"; NACA TM 1147; 1949.
- [5] Durvant, J.D., Erwin, J.R.: "Investigation of a Related Series of Turbine-Blade Profiles in Cascades"; NACA TN 3802, 1956.
- [6] Gopalakroshnan, S., Bozzola, R.: "A Numerical Technique for the Calculation of Transonic Flows in Turbomachinery Cascades"; ASME paper No. 71-FT-42; 1971.
- [7] Щегляев А. В. "Паровые Турбины"; Госэнергоиздат; 1956.
- [8] Дейч М. Е., Самойлович Г. С. "Основы Аэродинамики Осевых Турбин"; Машиз; 1956.
- [9] Liu Kao-Len, Shih Ming-Lum, and Wu Chun-Hua, "Aerodynamic Design and Analysis of Turbomachine," Journal of Mechanical Engineering, II, Vol. 1, 1963.
- [10] Paulon, J., Reboux, J., Sovrano, R.: "Comparison of Test Results Obtained on Plane and Annular, Fixed or Rotating Supersonic Blade Cascades"; Trans. ASME, Series A; Vol. 97, No. 2; 1975.
- [11] Wu Chun-hua, "The Solution of Compressible Flow Passing Through Cascades on an Arbitrary Revolving Surface and the Design of Such Cascades", Journal of Mechanical Engineering, 4, Vol. 1, 1956.
- [12] Tsay Ruey-shen, "The Design of Axial Flow Turbine Machinery Cascades on an Arbitrary Revolving Surface - Some Development in the Mean Stream Line Method (II)", Symposium on the aerodynamic thermodynamic calculation, design, and experience exchange in turbine machinery, 1977.

## APPENDIX A\*

In Appendix A, we briefly introduced the use of flow function expansion to obtain flow boundary and the analytical solution of the planar flow which is expanded in the normal direction of the stream line using the mean stream line method. It also explained that the analytical solution of the mean stream line method can also be used for compressor planar cascades with higher density.

### I. The Use of Flow Function To Solve for the Flow Boundary

For every  $z$  on the boundary of the flow in the cascade, the flow function has the relation  $d\psi = c_z dz$ . If we consider  $y$  as a function of  $\psi$   $y = y(\psi)$ , then

$$dy = d\psi / f_z \quad (A-1)$$

and

$$\Delta y = y - y_m = \left(\frac{\partial y}{\partial \psi}\right)_m \Delta \psi + \frac{1}{2!} \left(\frac{\partial^2 y}{\partial \psi^2}\right)_m \Delta \psi^2 + \frac{1}{3!} \left(\frac{\partial^3 y}{\partial \psi^3}\right)_m \Delta \psi^3 + \dots \quad (A-2)$$

The partial derivatives of  $y$  with respect to  $\psi$  in equation (A-12) can be obtained from equation (A-1) as:

$$\frac{\partial y}{\partial \psi} = \frac{1}{f_z} \quad (A-3)$$

$$\frac{\partial^2 y}{\partial \psi^2} = -\frac{1}{f_z^2} \frac{\partial f_z}{\partial \psi} \quad (A-4)$$

\*This appendix is mainly a combination of the graduation theses of some of the students (Liu Yen-hau, Yuen Chie-Quin, Lee Foo-ming, Wu Wen-ching, Yu Tso-chu, etc.) of the class of 59 in the department of modern mechanics at China Science and Technology University. Since it has never been published, it is included here.



$$\frac{\partial^2 \psi}{\partial y^2} = \frac{3}{2} \left( \frac{\partial^2 \psi}{\partial x^2} \right)^2 - \frac{1}{2} \frac{\partial^4 \psi}{\partial x^4} \quad (A-5)$$

Since the original mean stream line method only uses up to the second order derivatives  $\frac{\partial^2 \psi}{\partial x^2}$  to provide sufficient accuracy, therefore the flow function expansion is also used up to the  $\frac{\partial^2 \psi}{\partial x^2}$  term. Substituting the above three equations into (A-2), we then can obtain the equation of the flow boundary which can be solved directly:

$$\Delta y = \Delta y_1 - \frac{1}{2} \left( \frac{\partial^2 \psi}{\partial x^2} \right)_1 \Delta y_1^2 + \frac{1}{6} \left[ 3 \left( \frac{\partial^2 \psi}{\partial x^2} \right)_1^2 - \left( \frac{\partial^4 \psi}{\partial x^4} \right)_1 \right] \Delta y_1^3 + \dots \quad (A-6)$$

where  $\Delta y_1$  is the expansion distance when the flow is assumed to be a pure one-dimensional flow.

$$\Delta y_1 = \Delta \psi / c_{1,m} \quad (A-7)$$

Using this method to find the solution for the example in Reference [3] and comparing the result with that obtained originally using the third order algebraic equation method, we realized that the solutions obtained using these two methods are very close.

## II. The Method Used to Expand in the Normal Direction of the Selected Stream Line

The original mean stream line involves expansion in the y direction which is convenient in the calculation of planar cascades. If we establish a new coordinate system (l,n) at each expansion point (z,y) on the mean stream line where l is the tangential direction of the stream line and n is its normal direction with the direction defined as pointing from the center of curvature toward the stream line (See Figure A-1),

then it is possible to expand in the new coordinate  $n$  direction for each point. At this time the forms of the partial differential equations in Reference [3] are still valid with respect to the new coordinate systems. The only thing is that all the  $\beta_m$  values should be 0 looking from the new coordinates. In addition, the superscript ' should be considered as the partial derivative of  $l$  rather than  $z$ . The two derivatives should have the following relationships:

$$\frac{d}{dx} = \frac{dx'}{dx} \frac{d}{dx'} = \cos \theta \frac{d}{dx'} \quad (\text{A-8})$$

$$\frac{d^2}{dx^2} = \frac{d}{dx} \left( \frac{dx'}{dx} \right) \frac{d}{dx'} + \frac{dx'}{dx} \frac{d^2}{dx'^2} = -\sin \theta \frac{d}{dx'} + \cos \theta \frac{d^2}{dx'^2} \quad (\text{A-9})$$

Therefore of all the  $\frac{d}{dx}$ ,  $\frac{d^2}{dx^2}$  and  $\beta(z)$  are originally known, then it is possible to calculate all the  $\frac{d}{dx'}$  and  $\frac{d^2}{dx'^2}$ , based on the above two equations. Subsequently, they can be substituted into the partial differential equations in the  $n$  direction to find the solution. Actually since the  $\beta_m$  values are always zero in the new coordinate system, it is easier to obtain the partial differential equations with respect to the  $n$  direction than getting those in the  $y$  direction. It is shown as the following (where  $\Omega$  is the radius of curvature of the selected stream line).

$$\frac{1}{\Omega} \frac{\partial^2 \psi}{\partial n^2} = -\frac{1}{\Omega^2} (1 - M^2) \quad (\text{A-10})$$

$$\begin{aligned} \frac{1}{\Omega} \frac{\partial^3 \psi}{\partial n^3} = & \frac{1}{\Omega^2} [2 - 5M^2 + (2 - 3M^2)M^2] \\ & - \frac{1}{\Omega} \frac{\partial^2 \psi}{\partial n^2} (1 - M^2)^2 \\ & + \frac{1}{\Omega} \frac{\partial \psi}{\partial n} M^2 [1 - (1 - M^2)M^2 - 2M^4] \end{aligned} \quad (\text{A-11})$$

$$\frac{1}{\Omega} \frac{\partial \psi}{\partial n} = -\frac{1}{\Omega^2} \quad (\text{A-12})$$

$$\frac{1}{\Omega} \frac{\partial^2 \psi}{\partial n^2} = \frac{2}{\Omega^2} - \frac{1}{\Omega} \frac{\partial \psi}{\partial n} (1 - M^2) + \left( \frac{1}{\Omega} \frac{d\psi}{dx} \right)^2 (1 + M^2) \quad (\text{A-13})$$

In the determination of the flow function, it is desirable to use the same flow function expansion as in the previous equation also should be similar to that expansion as follows:

$$\Delta\eta = \frac{1}{2} \left[ \frac{\partial^2 \eta}{\partial \lambda^2} + \frac{\partial^2 \eta}{\partial n^2} \right] + \frac{1}{6} \left[ 3 \frac{\partial^3 \eta}{\partial \lambda^3} + 3 \frac{\partial^3 \eta}{\partial \lambda \partial n^2} + \frac{\partial^3 \eta}{\partial \lambda^2 \partial n} + \frac{\partial^3 \eta}{\partial \lambda \partial n^3} \right] \quad (A-14)$$

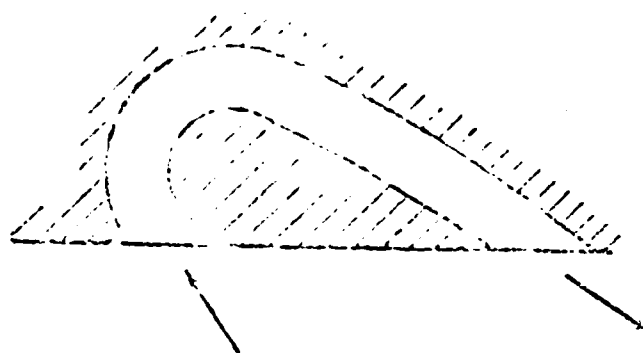
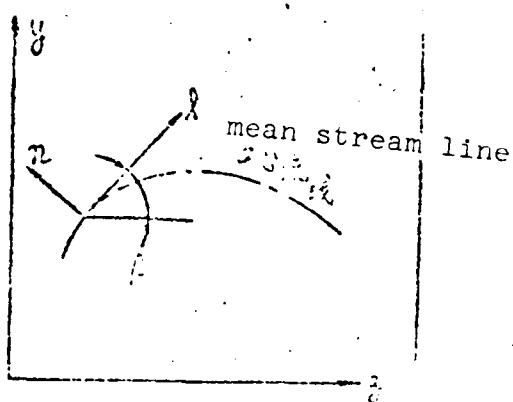


Figure A-1. l-n Coordinate system.

Figure A-2. The Boundary With the Return Flow Passing by.

The equation which determines the velocity distribution then becomes:

$$\lambda = \lambda_m \left[ 1 + \left( \frac{\partial \eta}{\partial \lambda} \right)^2 + \left( \frac{\partial \eta}{\partial n} \right)^2 + \dots \right] \quad (A-15)$$

If the normal direction expansion method is used to solve the planar cascade problem, although the calculation is less in the determination of partial derivatives, yet, because there is another transformation process to turn the flow boundary from the (l, n) coordinate system back to the original (Z, y) coordinate system, the total amount of calculation is not going

to be too much less. Furthermore, the normal direction expansion method makes it most difficult to calculate the velocity distribution in the most important inlet and outlet regions on the back arc. Therefore, it may not be suitable to use a pure normal direction expansion method. However, for some flow boundaries where the cross sections of the inlet and outlet are perpendicular to the mean stream line or where there is a large turn, it is better to use this method. For example, the boundary where the return flow passes by in a return flow turbine (See Figure A-2) is such a case. We have used this method to design the flow boundary of a natural gas expansion turbine. The preliminary result was satisfactory.

### III. The Feasibility of Using the Mean Stream Line Method to Calculate Axial Flow Compressor Planar Cascades

Reference [3] pointed out that it is possible to use the existing mean stream line method to design planar cascades of the axial flow compressors. In order to verify this view, we have actually solved a series of forward and reverse problems of this type of cascades. The forward problem is to find solutions for cascades with known velocity distributions such as the NACA 65 series and the NGTE C series cascades. The range of variation of the cascade density calculated is  $1.06 \sim 1.20$ . The range of variation in the geometric deflection angle of the blade profile is  $24.6^\circ \sim 65^\circ$ . The results obtained from the forward problem are more consistent to those obtained experimentally. This also means that for axial flow compressor planar cascades with higher density, it is still possible to find the solution using the existing mean stream line method and the first three terms of the Taylor series. It breaks the tradition that such a method was only able to be used in the calculation of turbine cascades.

## APPENDIX B

Appendix B gives all the expressions and numerical tables of the  $B_n(\beta)$  functions in equations (1) - (4) to be used during the course.

Table of functions used in the calculation

1	2	3	4	5	6	7
2						
3		4	4	5	4	5
	10000	10000	0	20000	0	
5°	00000	00000	00000	00000	00000	00000
10°	00000	00000	00000	00000	00000	00000
15°	00000	00000	00000	00000	00000	00000
20°	00000	00000	00000	00000	00000	00000
25°	00000	00000	00000	00000	00000	00000
30°	00000	00000	00000	00000	00000	00000
35°	00000	00000	00000	00000	00000	00000
40°	00000	00000	00000	00000	00000	00000
45°	00000	00000	00000	00000	00000	00000
50°	00000	00000	00000	00000	00000	00000
55°	00000	00000	00000	00000	00000	00000
60°	00000	00000	00000	00000	00000	00000
65°	00000	00000	00000	00000	00000	00000
70°	00000	00000	00000	00000	00000	00000
75°	00000	00000	00000	00000	00000	00000
80°	00000	00000	00000	00000	00000	00000

Table Cont'd.

$\hat{A}_j$	$P_j$	$Z_j$	$\hat{A}_j$	$P_j$	$Z_j$
0.85543	-0.09305	0.0000	0.85543	-0.09305	0.0000
1.6029	-0.20092	0.0000	1.6029	-0.20092	0.0000
2.1560	-0.0597	0.0000	2.1560	-0.0597	0.0000
2.4549	-0.0000	0.0000	2.4549	-0.0000	0.0000
2.4794	-0.2176	0.0000	2.4794	-0.2176	0.0000
2.2500	0	0.0000	2.2500	0	0.0000
1.0223	0.1700	0.0000	1.0223	0.1700	0.0000
1.2784	0.2934	0.0000	1.2784	0.2934	0.0000
0.7071	0.0000	0.0000	0.7071	0.0000	0.0000
0.1933	0.3578	0.0000	0.1933	0.3578	0.0000
-0.1984	0.2178	0.0000	-0.1984	0.2178	0.0000
-0.4330	0.2500	0.0000	-0.4330	0.2500	0.0000
-0.5087	0.1725	0.0000	-0.5087	0.1725	0.0000
-0.4538	0.1003	0.0000	-0.4538	0.1003	0.0000
-0.3109	0.0000	0.0000	-0.3109	0.0000	0.0000
-0.1658	0.0000	0.0000	-0.1658	0.0000	0.0000

1	2	3	4	5	6
1	1	1	1	1	1
2	1	1	1	1	1
3	1	1	1	1	1
4	1	1	1	1	1
5	1	1	1	1	1
6	1	1	1	1	1
7	1	1	1	1	1
8	1	1	1	1	1
9	1	1	1	1	1
10	1	1	1	1	1
11	1	1	1	1	1
12	1	1	1	1	1
13	1	1	1	1	1
14	1	1	1	1	1
15	1	1	1	1	1
16	1	1	1	1	1
17	1	1	1	1	1
18	1	1	1	1	1
19	1	1	1	1	1
20	1	1	1	1	1
21	1	1	1	1	1
22	1	1	1	1	1
23	1	1	1	1	1
24	1	1	1	1	1
25	1	1	1	1	1
26	1	1	1	1	1
27	1	1	1	1	1
28	1	1	1	1	1
29	1	1	1	1	1
30	1	1	1	1	1
31	1	1	1	1	1
32	1	1	1	1	1
33	1	1	1	1	1
34	1	1	1	1	1
35	1	1	1	1	1
36	1	1	1	1	1
37	1	1	1	1	1
38	1	1	1	1	1
39	1	1	1	1	1
40	1	1	1	1	1
41	1	1	1	1	1
42	1	1	1	1	1
43	1	1	1	1	1
44	1	1	1	1	1
45	1	1	1	1	1
46	1	1	1	1	1
47	1	1	1	1	1
48	1	1	1	1	1
49	1	1	1	1	1
50	1	1	1	1	1
51	1	1	1	1	1
52	1	1	1	1	1
53	1	1	1	1	1
54	1	1	1	1	1
55	1	1	1	1	1
56	1	1	1	1	1
57	1	1	1	1	1
58	1	1	1	1	1
59	1	1	1	1	1
60	1	1	1	1	1
61	1	1	1	1	1
62	1	1	1	1	1
63	1	1	1	1	1
64	1	1	1	1	1
65	1	1	1	1	1
66	1	1	1	1	1
67	1	1	1	1	1
68	1	1	1	1	1
69	1	1	1	1	1
70	1	1	1	1	1
71	1	1	1	1	1
72	1	1	1	1	1
73	1	1	1	1	1
74	1	1	1	1	1
75	1	1	1	1	1
76	1	1	1	1	1
77	1	1	1	1	1
78	1	1	1	1	1
79	1	1	1	1	1
80	1	1	1	1	1
81	1	1	1	1	1
82	1	1	1	1	1
83	1	1	1	1	1
84	1	1	1	1	1
85	1	1	1	1	1
86	1	1	1	1	1
87	1	1	1	1	1
88	1	1	1	1	1
89	1	1	1	1	1
90	1	1	1	1	1
91	1	1	1	1	1
92	1	1	1	1	1
93	1	1	1	1	1
94	1	1	1	1	1
95	1	1	1	1	1
96	1	1	1	1	1
97	1	1	1	1	1
98	1	1	1	1	1
99	1	1	1	1	1
100	1	1	1	1	1



Table Cont'd.

$E_0$	$E_1$	$E_2$	$E_3$	$E_4$	$E_5$
0.0000	0.0000	0.0000	0.0000	0.0000	0.0000
0.5	0.5	0.4	0.4	0.4	0.4
0	0	0.0000	1.0000	1.0000	-1.0000
0.0000	-1.7128	0.0000	0.0000	0.0000	-0.0000
0.1000	-3.2000	1.7128	0.0000	0.0000	-0.0000
0.2000	-4.4000	1.0000	0.2000	0.2000	-0.0000
0.3000	-5.2000	1.1000	-0.1000	0.7000	-0.0000
0.4000	-5.5000	0.8000	-0.3000	0.4000	0.0000
0.5000	-5.3000	0.4000	-0.5000	0.1000	0.0000
0.6000	-4.6000	0.0000	-0.6000	0.0000	0.0000
0.7000	-3.4000	-0.0000	-0.4000	0.0000	0.0000
0.8000	-1.9000	-0.2000	-0.1000	0.0000	0.0000
0.9000	0.0000	-0.4000	0.0000	0.0000	0.0000
1.0000	1.0000	0.0000	0.0000	0.0000	0.0000
1.1000	2.0000	0.0000	0.0000	0.0000	0.0000
1.2000	3.0000	0.0000	0.0000	0.0000	0.0000
1.3000	4.0000	0.0000	0.0000	0.0000	0.0000
1.4000	5.0000	0.0000	0.0000	0.0000	0.0000
1.5000	6.0000	0.0000	0.0000	0.0000	0.0000
1.6000	7.0000	0.0000	0.0000	0.0000	0.0000
1.7000	8.0000	0.0000	0.0000	0.0000	0.0000
1.8000	9.0000	0.0000	0.0000	0.0000	0.0000
1.9000	10.0000	0.0000	0.0000	0.0000	0.0000
2.0000	11.0000	0.0000	0.0000	0.0000	0.0000
2.1000	12.0000	0.0000	0.0000	0.0000	0.0000
2.2000	13.0000	0.0000	0.0000	0.0000	0.0000
2.3000	14.0000	0.0000	0.0000	0.0000	0.0000
2.4000	15.0000	0.0000	0.0000	0.0000	0.0000
2.5000	16.0000	0.0000	0.0000	0.0000	0.0000
2.6000	17.0000	0.0000	0.0000	0.0000	0.0000
2.7000	18.0000	0.0000	0.0000	0.0000	0.0000
2.8000	19.0000	0.0000	0.0000	0.0000	0.0000
2.9000	20.0000	0.0000	0.0000	0.0000	0.0000
3.0000	21.0000	0.0000	0.0000	0.0000	0.0000

Key: (1) Function, 2. Equation, 3. Functional Characteristics, 4. Even, 5. Odd.

SCIENTIFIC TECHNOLOGICAL RESEARCH REPORT

THEORY OF THREE-DIMENSIONAL FLOW IN TRANSONIC  
TURBINE MACHINERY WITH SHOCK WAVE INTERRUPTIONS

THE 5TH RESEARCH OFFICE OF THE INSTITUTE OF MECHANICS  
CHINESE ACADEMY OF SCIENCE  
OCTOBER 20, 1978

THEORY OF THREE-DIMENSIONAL FLOW IN TRANSONIC TURBINE  
MACHINERY WITH SHOCK WAVE INTERRUPTIONS

(Preliminary Manuscript)

Hsu Tsen-chung

October 20, 1978

# THEORY OF THREE-DIMENSIONAL FLOW IN TRANSONIC TURBINE MACHINERY WITH SHOCK WAVE INTERRUPTIONS

Hsu Tsen-chung

## ABSTRACT

In order to be consistent with the three-dimensional spatial flow in turbine machinery with shock waves, this paper derives the "four-dimensional" basic equations of the  $S_1$  and  $S_2$  flow surfaces through the extension of the flow surface concept to the unsteady flow condition. They are also applicable to spatial three-dimensional unsteady flow. Using the theory of the characteristic line for these equations, we can obtain the mutual relationships between the characteristics. From them, we can determine the boundary conditions of the steady flow. These basic equations, boundary conditions and applicable initial conditions can completely establish the transonic flow problem with shock waves for both types of the flow surfaces. Thus, based on the procedures recommended in this paper to obtain the complete solution of the three-dimensional flow and by choosing the proper difference equations, the numerical solution can then be obtained.

## I. INTRODUCTION

In order to obtain the solution of three-dimensional flow in subsonic and supersonic turbine machinery, [1] presented the  $S_1$  and  $S_2$  relative flow surface theory to establish the basic equations and boundary conditions on these two types of flow surfaces and also presented procedures to solve these equations. For over 20 years, this theory has been widely used. This practice indicates that this two flow surface theory is not only the calculation method for three-dimensional flow in the turbine machinery, but also the theoretical basis of the design method of such machinery. The calculation and iteration processes of the two types of flow surfaces

are not only the procedures to solve the three-dimensional flow problem, but also those to design three-dimensional flow turbine machinery.

Recently, with the development of transonic turbine machinery, there has been a desperate need to calculate three-dimensional flow with shock wave interruptions. In [2], it was pointed out, after the establishment of the basic equations of three-dimensional flow and the integral form on the two kinds of flow surfaces and the derivation of the relations of parameters in front and behind the shock wave under various conditions, that in order to solve the three-dimensional flow problem we must calculate a two-dimensional flow which is consistent with the three-dimensional flow on each of the two surfaces, and carry out iterations between the calculations of the two surfaces.

The establishment of this type of two-dimensional flow is a fixed solution problem. Based on the results in [2], it cannot be carried out on an assigned flow surface. It must extend the steady flow surface model presented in [1] to the unsteady flow condition\*. It transforms three-dimensional flow to the two types of flow surfaces which vary with time. This paper first briefly introduces this unsteady surface and the geometric relations on it. It also shows the relation between three-dimensional flow surfaces at every instance.

It is then followed, in the second and third sections of this paper, by the establishment of the basic equations on the two flow surfaces which are consistent with the three-dimensional flow. They are applicable in the solution of the unsteady flow and the calculation of steady flow with shock waves.

---

\* Comrade Huang Ray Tsien has pointed out that it is possible to extend the steady flow surface to the unsteady flow surface.

In the fourth section of this paper, the characteristic relations on the two types of surfaces are derived on the basis of characteristic line theory. It presents the boundary conditions at upstream and downstream boundaries and on the flow surfaces which are suitable for solving the problem of steady flow with shock waves. The initial conditions can be given using the usual method. Thus, this specific solution problem can be completely established.

Finally, in the fifth section of this paper we briefly describe the procedures used to solve the three-dimensional flow problem by iteration of calculations between the two types of unsteady flow surfaces.

## II. UNSTEADY FLOW SURFACE AND ITS GEOMETRIC RELATION

The combination of all the stream lines of all the points on a curve in the flow field which is a stream line forms the spatial flow surface.

In unsteady flow, the flow surface varies with time. Therefore, in the four-dimensional space including time, the flow surface can be expressed as:

$$\bar{S}(r, \varphi, z, t) = 0$$

Thus

$$\frac{\partial \bar{S}}{\partial r} dr + \frac{\partial \bar{S}}{\partial \varphi} d\varphi + \frac{\partial \bar{S}}{\partial z} dz + \frac{\partial \bar{S}}{\partial t} dt = 0$$

The unit vector in the normal direction  $\vec{N}(N_r, N_u, N_z, N_t)$  satisfies

$$\frac{N_r}{\frac{\partial \bar{S}}{\partial r}} = \frac{N_u}{\frac{1}{r} \frac{\partial \bar{S}}{\partial \varphi}} = \frac{N_z}{\frac{\partial \bar{S}}{\partial z}} = \frac{N_t}{\frac{1}{U} \frac{\partial \bar{S}}{\partial t}} = \frac{1}{\sqrt{\left(\frac{\partial \bar{S}}{\partial r}\right)^2 + \left(\frac{1}{r} \frac{\partial \bar{S}}{\partial \varphi}\right)^2 + \left(\frac{\partial \bar{S}}{\partial z}\right)^2 + \left(\frac{1}{U} \frac{\partial \bar{S}}{\partial t}\right)^2}}$$

Therefore, on the four-dimensional flow surface:

$$N_r dr + N_u r d\varphi + N_z dz + N_t U dt = 0$$

$$\frac{N_t}{N_r} = -\frac{1}{U} \frac{\partial r}{\partial t}, \quad \frac{N_t}{N_u} = -\frac{r}{U} \frac{\partial \varphi}{\partial t} \quad (1)$$

On the other hand, there is a flow surface at any instance in the space

$$S(r, \varphi, z) = 0$$

Its unit vector  $\vec{n}(n_r, n_u, n_z)$  is a function of time  $t$  and it satisfies

$$\frac{n_r}{\frac{\partial S}{\partial r}} = \frac{n_u}{r \frac{\partial S}{\partial \varphi}} = \frac{n_z}{\frac{\partial S}{\partial z}} = \frac{1}{\sqrt{\left(\frac{\partial S}{\partial r}\right)^2 + \left(r \frac{\partial S}{\partial \varphi}\right)^2 + \left(\frac{\partial S}{\partial z}\right)^2}}$$

In the meantime, from the definition of the flow surface, for every instance we have

$$\vec{n} \cdot \vec{W} = 0$$

which is

$$n_r W_r + n_u W_u + n_z W_z = 0$$

It should be pointed out that the corresponding components of the three-dimensional and four-dimensional unit normal direction vectors  $\vec{n}$  and  $\vec{N}$  are not equal, but there are the following relations:

$$\frac{N_u}{N_r} = \frac{n_u}{n_r}, \quad \frac{N_z}{N_r} = \frac{n_z}{n_r}, \quad \frac{N_t}{N_u} = \frac{n_t}{n_u} \quad (2)$$

With the above relations on the unsteady flow surface, we can transform the basic equations of the non-viscous gas in a relative coordinate system which is rotating at a constant angular velocity as shown in [1]:

$$\frac{\partial \rho}{\partial t} + \frac{1}{r} \frac{\partial (\rho w_r r)}{\partial r} + \frac{1}{r} \frac{\partial (\rho w_\varphi)}{\partial \varphi} + \frac{\partial (\rho w_z)}{\partial z} = 0 \quad (3)$$

$$\frac{\partial w_r}{\partial t} + w_r \frac{\partial w_r}{\partial r} + \frac{w_\varphi}{r} \frac{\partial w_r}{\partial \varphi} + w_z \frac{\partial w_r}{\partial z} - \frac{v_\varphi^2}{r} = -\frac{1}{\rho} \frac{\partial p}{\partial r} \quad (4)$$

$$\frac{\partial w_\varphi}{\partial t} + w_r \frac{\partial w_\varphi}{\partial r} + \frac{w_\varphi}{r} \frac{\partial w_\varphi}{\partial \varphi} + w_z \frac{\partial w_\varphi}{\partial z} + \frac{w_r w_\varphi}{r} + 2w_r w_z = -\frac{1}{\rho r} \frac{\partial p}{\partial \varphi} \quad (5)$$

$$\frac{\partial w_z}{\partial t} + w_r \frac{\partial w_z}{\partial r} + \frac{w_\varphi}{r} \frac{\partial w_z}{\partial \varphi} + w_z \frac{\partial w_z}{\partial z} = -\frac{1}{\rho} \frac{\partial p}{\partial z} \quad (6)$$

$$\frac{\partial I}{\partial t} + w_r \frac{\partial I}{\partial r} + \frac{w_\varphi}{r} \frac{\partial I}{\partial \varphi} + w_z \frac{\partial I}{\partial z} - \frac{1}{\rho} \frac{\partial p}{\partial t} = 0 \quad (7)$$

separately to the two types of unsteady flow surface. It should be pointed out that, as a closed series of equations, the equation of the state of the gas and other relations should be included in addition to the above equations.

$$p = \rho R T \quad (8)$$

and

$$dh = c_p dT \quad I = h + \frac{w^2}{2} - \frac{U^2}{1} \quad (9)$$

Because these algebraic equations maintain their forms on the flow surface, they will not be described further in the following sections.

### III. BASIC EQUATIONS ON THE UNSTEADY FLOW SURFACE $\bar{S}_1$

Let us consider the unsteady flow surface formed by the stream lines passing through a certain circle located upstream of the cascade.

$$\bar{S}_1(r, \varphi, z, t) = 0$$



Any arbitrary function  $q$  on it can be expressed as

$$q = q(r, \varphi, z, t) = q[r(\varphi, z, t), \varphi, z, t]$$

By noting Equation (2), the partial derivatives of  $q$  on the four-dimensional flow surface can be written as

$$\begin{aligned} \frac{1}{r} \frac{\partial q}{\partial \varphi} &= \frac{1}{r} \frac{\partial q}{\partial \varphi} - \frac{n_u}{n_r} \frac{\partial q}{\partial r} \\ \frac{\partial q}{\partial z} &= \frac{\partial q}{\partial z} - \frac{n_z}{n_r} \frac{\partial q}{\partial r} \\ \frac{\partial q}{\partial t} &= \frac{\partial q}{\partial t} - \frac{UN_r}{N_r} \frac{\partial q}{\partial r} \end{aligned}$$

From these relations, Equation (3) can be rewritten as

$$\frac{\partial \rho}{\partial t} + \frac{1}{r} \frac{\partial (\rho W_u)}{\partial \varphi} + \frac{\partial (\rho W_z)}{\partial z} = \rho C(\varphi, z, t)$$

where

$$C(\varphi, z, t) = -\frac{1}{n_r} \left[ \frac{n_r}{r} \frac{\partial (W_r)}{\partial r} + n_u \frac{\partial W_u}{\partial r} + n_z \frac{\partial W_z}{\partial r} \right] - \frac{UN_r}{N_r} \frac{\partial \ln \rho}{\partial r} \quad (10)$$

By introducing

$$\frac{d \ln b}{dt} = -C + \frac{n_z}{n_r} \frac{W_z}{r} \quad (11)$$

the continuity equation can be expressed as

$$\frac{\partial (b \rho)}{\partial t} + \frac{1}{r} \frac{\partial (b \rho W_u)}{\partial \varphi} + \frac{1}{r} \frac{\partial (r b \rho W_z)}{\partial z} = 0 \quad (12)$$

Similarly, Equations (4)-(7) can be respectively expressed as

AD-A105 607

FOREIGN TECHNOLOGY DIV WRIGHT-PATTERSON AFB OH  
AIR BREATHING PROPULSION RESEARCH (SELECTED ARTICLES), (U)  
SEP 81 R TSAY, T HSU  
FTD-ID(RS)T-0354-81

F/6 20/4

UNCLASSIFIED

2 OF 2

ALL A  
U-60



END  
DATE  
FILMED

11-81  
DTIC

$$\frac{\partial w_r}{\partial t} + \frac{w_u}{r} \frac{\partial w_r}{\partial \varphi} + w_z \frac{\partial w_r}{\partial z} - \frac{w_u^2}{r} = f_r' \quad (13)$$

$$\frac{\partial w_u}{\partial t} + \frac{w_u}{r} \frac{\partial w_u}{\partial \varphi} + w_z \frac{\partial w_u}{\partial z} + \frac{w_r w_u}{r} + 2\omega w_r = -\frac{1}{s} \frac{\partial p}{\partial \varphi} + f_u' \quad (14)$$

$$\frac{\partial w_z}{\partial t} + \frac{w_u}{r} \frac{\partial w_z}{\partial \varphi} + w_z \frac{\partial w_z}{\partial z} = -\frac{1}{s} \frac{\partial p}{\partial z} + f_z' \quad (15)$$

$$\frac{\partial I}{\partial t} + \frac{w_u}{r} \frac{\partial I}{\partial \varphi} + w_z \frac{\partial I}{\partial z} - \frac{1}{s} \frac{\partial p}{\partial r} = J \quad (16)$$

where

$$\vec{f}' = -\frac{1}{\mu s} \frac{\partial p}{\partial r} \vec{n} - \frac{U N_r}{N_r} \frac{\partial \vec{w}}{\partial r}$$

$$J = \frac{U N_r}{N_r} \left( \frac{\partial I}{\partial r} - \frac{1}{s} \frac{\partial p}{\partial r} \right)$$

Equations (13)-(15) can also be expressed using I and S:

$$\frac{\partial w_r}{\partial t} + \frac{w_u}{r} \frac{\partial w_r}{\partial \varphi} + w_z \frac{\partial w_r}{\partial z} - \frac{w_u^2}{r} - 2\omega w_u = f_r$$

$$\frac{\partial w_u}{\partial t} + \frac{w_u}{r} \frac{\partial w_u}{\partial \varphi} + w_z \left( \frac{1}{r} \frac{\partial w_z}{\partial \varphi} - \frac{\partial w_u}{\partial z} \right) + \frac{w_r w_u}{r} + 2\omega w_r = -\frac{1}{r} \frac{\partial I}{\partial \varphi} + \frac{T}{r} \frac{\partial S}{\partial \varphi} + f_u$$

$$\frac{\partial w_z}{\partial t} - w_r \frac{\partial w_z}{\partial z} + w_u \left( \frac{1}{r} \frac{\partial w_z}{\partial \varphi} - \frac{\partial w_u}{\partial z} \right) = -\frac{\partial I}{\partial z} + T \frac{\partial S}{\partial z} + f_z$$

$$\vec{f} = -\frac{1}{\mu} \left( \frac{\partial p}{\partial r} - T \frac{\partial S}{\partial r} - \omega^2 r \right) \vec{n} - \frac{U N_r}{N_r} \frac{\partial \vec{w}}{\partial r}$$

If we are considering a steady flow, the flow surface does not vary with time. In the above equations  $\frac{\partial}{\partial t} = 0$ ,  $N_r = 0$ . Then these equations can be transformed into the basic equations of the steady flow surface corresponding to Equations (34b), (40),

(41), (39a), (39b) and (39c) in [1]. In other words, comparing to the equations on the steady  $S_1$  flow surface, in the equations on the unsteady flow surface, besides the additional  $\frac{U M_\infty}{N_r} \frac{\partial \ln \xi}{\partial r}$  and  $\frac{U M_\infty}{N_r} \frac{\partial \eta}{\partial r}$  in the expressions of  $c$  and  $\bar{f}$  respectively. In the energy equation, there is a similar  $J$  term.

We found that, different from the basic equation of transonic flow with shock wave interruptions on the  $S_1$  flow surface used to date, in Equations (12)-(16)  $b$  varies with time and appears in the  $\frac{\partial}{\partial t}$  term. Simultaneously, it shows the effect of unsteady factors in  $\bar{f}$  and  $J$ . These are because of the use of the four-dimensional steady flow surface model in the derivation of these equations which are consistent with the spatial shock wave.

Considering the process of finding for a complete numerical solution, it is more accurate to carry out the calculation of the difference format in the invariance form during the interruption due to the shock waves. We can transform Equations (12)-(16) into the following divergent forms (or still called the invariance forms)

$$\frac{\partial(b\bar{f})}{\partial t} + \frac{1}{r} \frac{\partial(b\bar{n})}{\partial \varphi} + \frac{\partial(b\bar{q})}{\partial \xi} + \frac{b\bar{m}}{r} + \frac{n_u}{n_r} \frac{b\bar{n}}{r} = 0 \quad (18)$$

$$\frac{\partial(b\bar{m})}{\partial t} + \frac{1}{r} \frac{\partial}{\partial \varphi} \left( b \frac{m\bar{n}}{\xi} \right) + \frac{\partial}{\partial \xi} \left( b \frac{m\bar{q}}{\xi} \right) + b \left[ \frac{m^2}{\xi r} + \frac{n_u}{n_r} \frac{m\bar{n}}{\xi r} - \frac{\xi}{r} \left( \frac{n}{\xi} + \omega r \right)^2 - \xi f'_r \right] = 0 \quad (19)$$

$$\frac{\partial(b\bar{n})}{\partial t} + \frac{1}{r} \frac{\partial}{\partial \varphi} \left[ b \left( p + \frac{n^2}{\xi} \right) \right] + \frac{\partial}{\partial \xi} \left( b \frac{n\bar{q}}{\xi} \right) - \frac{p}{r} \frac{\partial b}{\partial \varphi} + b \left( \frac{m\bar{n}}{\xi r} + \omega m + \frac{n_u}{n_r} \frac{n^2}{\xi r} - \xi f'_u \right) = 0 \quad (20)$$

$$\frac{\partial(b\bar{q})}{\partial t} + \frac{1}{r} \frac{\partial}{\partial \varphi} \left( b \frac{n\bar{q}}{\xi} \right) + \frac{\partial}{\partial \xi} \left[ b \left( p + \frac{q^2}{\xi} \right) \right] - \frac{p}{r} \frac{\partial b}{\partial \xi} + b \left( \frac{n\bar{q}}{\xi r} + \frac{n_u}{n_r} \frac{n\bar{q}}{\xi r} - \xi f'_q \right) = 0 \quad (21)$$

$$\frac{\partial(b\bar{h})}{\partial t} + \frac{p}{r} \frac{\partial b}{\partial t} + \frac{1}{r} \frac{\partial}{\partial \varphi} \left[ b \bar{n} \frac{(H+p)}{\xi} \right] + \frac{\partial}{\partial \xi} \left[ b \bar{q} \frac{(H+p)}{\xi} \right] + \frac{b}{r} \left( m + \frac{n_u}{n_r} n \right) \frac{(H+p)}{\xi} + b \bar{e} = 0 \quad (22)$$

or

$$\frac{\partial(b\rho I)}{\partial t} - b \frac{\partial p}{\partial t} + \frac{1}{r} \frac{\partial(b\eta I)}{\partial \varphi} + \frac{\partial(l\ell I)}{\partial z} + bI \left( \frac{n}{r} + \frac{\eta_u}{\eta_r} \frac{n}{r} \right) + b\rho J = 0 \quad (22')$$

where

$$m = \rho W_r \quad (23)$$

$$n = \rho W_u \quad (24)$$

$$\ell = \rho W_z \quad (25)$$

$$H = \rho \left( e + \frac{W^2}{2} - \frac{U^2}{2} \right) = \rho \left( I - \frac{p}{\rho} \right) \quad (26)$$

$$\xi = -\frac{U\eta_r}{N_r} \left[ (H+p) \frac{\partial \rho \eta}{\partial r} - \frac{\partial H}{\partial r} \right] \quad (27)$$

#### IV. BASIC EQUATION ON THE UNSTEADY FLOW SURFACE $\bar{S}_2$

Let us consider the unsteady flow surface formed by stream lines passing through a radial line located upstream of the cascade.

$$\bar{S}_2(r, \varphi, z, t) = 0$$

Any arbitrary function  $q$  on it can be expressed as

$$q = q(r, \varphi, z, t) = q[r, \varphi(r, z, t), z, t]$$

By taking Equation (2) into consideration, the partial derivatives of  $q$  on the four-dimensional flow surface can be transformed as:

$$\begin{aligned}\frac{\partial \rho}{\partial r} &= \frac{\partial \rho}{\partial r} - \frac{n_r'}{n_u' r} \frac{\partial \rho}{\partial \varphi} \\ \frac{\partial \rho}{\partial z} &= \frac{\partial \rho}{\partial z} - \frac{n_z'}{n_u' r} \frac{\partial \rho}{\partial \varphi} \\ \frac{\partial \rho}{\partial t} &= \frac{\partial \rho}{\partial t} - \frac{\omega n_z'}{n_u'} \frac{\partial \rho}{\partial \varphi}\end{aligned}$$

From these relations, Equation (3) can be expressed as:

$$\frac{\partial \rho}{\partial t} + \frac{1}{r} \frac{\partial (\rho w_r r)}{\partial r} + \frac{\partial (\rho w_z)}{\partial z} = \rho c'(r, z, t)$$

where

$$c'(r, z, t) = -\frac{1}{n_u' r} \left( n_r' \frac{\partial w_r}{\partial \varphi} + n_u' \frac{\partial w_z}{\partial \varphi} + n_z' \frac{\partial w_z}{\partial \varphi} \right) - \frac{\omega n_z'}{n_u'} \frac{\partial \rho}{\partial \varphi} \quad (28)$$

by introducing

$$\frac{\partial \rho b'}{\partial t} = -c' + \frac{w_z}{r} \quad (29)$$

the continuity equation can be rewritten as:

$$\frac{\partial (\rho b')}{\partial t} + \frac{\partial (\rho w_r)}{\partial r} + \frac{\partial (\rho w_z)}{\partial z} = 0 \quad (30)$$

Similarly, Equations (4)-(7) are as the following respectively:

$$\frac{\partial w_r}{\partial t} + w_r \frac{\partial w_r}{\partial r} + w_z \frac{\partial w_r}{\partial z} - \frac{v_u^2}{r} = \frac{1}{\rho} \frac{\partial p}{\partial r} + F_r \quad (31)$$

$$\frac{\partial w_u}{\partial t} + w_r \frac{\partial w_u}{\partial r} + w_z \frac{\partial w_u}{\partial z} + \frac{w_r w_u}{r} + 2\omega w_r = F_u \quad (32)$$

$$\frac{\partial w_z}{\partial t} + w_r \frac{\partial w_z}{\partial r} + w_z \frac{\partial w_z}{\partial z} = -\frac{1}{\rho} \frac{\partial p}{\partial z} + F_z \quad (33)$$

$$\frac{\partial I}{\partial t} - \frac{1}{\rho} \frac{\partial p}{\partial t} + w_r \frac{\partial I}{\partial r} + w_z \frac{\partial I}{\partial z} = J' \quad (34)$$

where

$$\begin{aligned}\vec{F} &= -\frac{1}{N_u r} \frac{1}{\rho} \frac{\partial p}{\partial \varphi} \vec{n}' - \frac{\omega N_u'}{N_u} \frac{\partial \vec{w}}{\partial \varphi} \\ J' &= -\frac{\omega N_u'}{N_u} \left( \frac{\partial I}{\partial \varphi} - \frac{1}{\rho} \frac{\partial b}{\partial \varphi} \right)\end{aligned}\quad (35)$$

If we use I and S to express it, then the momentum equation can be transformed into:

$$\begin{aligned}\frac{\partial w_r}{\partial t} - \frac{w_u}{r} \frac{\partial (V_u r)}{\partial r} + w_z \left( \frac{\partial w_r}{\partial z} - \frac{\partial w_z}{\partial r} \right) &= -\frac{\partial I}{\partial r} + T \frac{\partial S}{\partial r} + F_r \\ \frac{d(V_u r)}{dt} &= F_u r \\ \frac{\partial w_z}{\partial t} - w_r \left( \frac{\partial w_r}{\partial z} - \frac{\partial w_z}{\partial r} \right) - \frac{w_u}{r} \frac{\partial (V_u r)}{\partial z} &= -\frac{\partial I}{\partial z} + T \frac{\partial I}{\partial z} + F_z\end{aligned}$$

Similarly to the situation on the  $S_1$  flow surface, in the steady flow the above equations can be transformed into equations (100), (98), (99a), (96a), (96b) and (96c) in [1], respectively. The difference between the steady and unsteady  $S_2$  flow surfaces is also the same as the situation for the  $S_1$  flow surface.

Equations (30)-(34) can be transformed into the divergent forms:

$$\frac{\partial (b' \rho)}{\partial t} + \frac{\partial (b' m)}{\partial r} + \frac{\partial (b' l)}{\partial z} = 0 \quad (36)$$

$$\frac{\partial (b' m)}{\partial t} + \frac{\partial}{\partial r} \left[ b' \left( \rho + \frac{m^2}{\rho} \right) \right] + \frac{\partial}{\partial z} \left( b' \frac{m l}{\rho} \right) - \rho \frac{\partial b'}{\partial r} - b' \rho \left( \frac{V_u^2}{r} + F_r \right) = 0 \quad (37)$$

$$\frac{\partial (b' m)}{\partial t} + \frac{\partial}{\partial r} \left( b' \frac{m m}{\rho} \right) + \frac{\partial}{\partial z} \left( b' \frac{m l}{\rho} \right) + b' \left( \frac{m m}{\rho r} + 2 \omega m - \rho F_u \right) = 0 \quad (38)$$

$$\frac{\partial (b' l)}{\partial t} + \frac{\partial}{\partial r} \left( b' \frac{m l}{\rho} \right) + \frac{\partial}{\partial z} \left[ b' \left( \rho + \frac{l^2}{\rho} \right) \right] - \rho \frac{\partial b'}{\partial r} - b' \rho F_z = 0 \quad (39)$$

$$\frac{\partial (b' l)}{\partial t} + \rho \frac{\partial b'}{\partial t} + \frac{\partial}{\partial r} \left[ b' m \frac{(H+P)}{\rho} \right] + \frac{\partial}{\partial z} \left[ b' l \frac{(H+P)}{\rho} \right] + b' \xi = 0 \quad (40)$$

or 
$$\frac{\partial(b\rho I)}{\partial t} - b' \frac{\partial p}{\partial t} + \frac{\partial(b'mI)}{\partial r} + \frac{\partial(b'lI)}{\partial z} + b' \rho J' = 0 \quad (40a)$$

where

$$E' = -\frac{\omega N_u'}{N_u'} \left[ (H+p) \frac{\partial \ln p}{\partial \varphi} - \frac{\partial H}{\partial \varphi} \right] \quad (41)$$

It should be pointed out that the basic equations on the two types of unsteady flow surfaces are applicable in slowing the unsteady flow as well as the steady flow with shock waves. The difference in the two specific solution problems is in their boundary conditions.

#### V. BOUNDARY CONDITIONS AND INITIAL CONDITIONS

In the two previous sections, we have already established the hyperbolic partial differential equations on the two types of unsteady flow surfaces. The following is a presentation of the corresponding boundary conditions and initial conditions.

In the calculation of the initial value-boundary value problems, the parameters on the surfaces and at the upstream and downstream boundaries are related to the parameters of the flow a moment before. Thus, we should use the characteristic line theory [3] of the hyperbolic equations to derive the relative relations between the characteristics in order to determine the boundary conditions [4,5,6,7].

##### (I) The boundary condition on the $S_1$ flow surface

At this time we can obtain the following relations:

此时可得出以下的相容关系

$$\frac{\partial p}{\partial t} + \frac{w_u}{r} \frac{\partial p}{\partial \varphi} + w_s \frac{\partial p}{\partial z} - a^2 \left( \frac{\partial p}{\partial t} + \frac{w_u}{r} \frac{\partial p}{\partial \varphi} + w_s \frac{\partial p}{\partial z} \right) = \frac{UM}{N_r} \left( a^2 \frac{\partial p}{\partial r} - \frac{\partial p}{\partial r} \right) \quad (42)$$

$$\sin \mu \left( \frac{\partial w_u}{\partial t} + \frac{w_u}{r} \frac{\partial w_u}{\partial \varphi} + w_s \frac{\partial w_u}{\partial z} + \frac{1}{r} \frac{\partial p}{\partial \varphi} \right) - \cos \mu \left( \frac{\partial w_u}{\partial t} + \frac{w_u}{r} \frac{\partial w_u}{\partial \varphi} + w_s \frac{\partial w_u}{\partial z} + \frac{1}{r} \frac{\partial p}{\partial \varphi} \right) =$$

$$= f_2' \sin \mu - \left( f_u' - \frac{w_u w_u}{r} - 2\omega w_r \right) \cos \mu \quad (43)$$



$$\begin{aligned}
& -\frac{\partial p}{\partial t} + (w_u + a \sin \mu) \frac{1}{r} \frac{\partial p}{\partial \varphi} + (w_z + a \cos \mu) \frac{\partial p}{\partial z} + \rho a \left( \sin \mu \frac{\partial w_u}{\partial t} + \cos \mu \frac{\partial w_z}{\partial t} \right) + \\
& + \rho a \left[ (w_u \sin \mu + a) \frac{1}{r} \frac{\partial w_u}{\partial \varphi} + (w_z \cos \mu + a) \frac{\partial w_z}{\partial z} + w_u \sin \mu \frac{\partial w_u}{\partial \varphi} + \frac{w_u}{r} \cos \mu \frac{\partial w_z}{\partial \varphi} \right] = \\
& = \rho a^2 c + \rho a (f'_z \cos \mu + f'_u \sin \mu) - \rho a w_r \left( \frac{w_u}{r} + 2\omega \right) \sin \mu + \frac{U M_z}{N_r} \left( a^2 \frac{\partial p}{\partial r} - \frac{\partial p}{\partial r} \right) \quad (44)
\end{aligned}$$

$$\begin{aligned}
& -\frac{\partial p}{\partial t} + (w_u - a \sin \mu) \frac{1}{r} \frac{\partial p}{\partial \varphi} + (w_z - a \cos \mu) \frac{\partial p}{\partial z} - \rho a \left( \sin \mu \frac{\partial w_u}{\partial t} + \cos \mu \frac{\partial w_z}{\partial t} \right) - \\
& - \rho a \left[ (w_u \sin \mu - a) \frac{1}{r} \frac{\partial w_u}{\partial \varphi} + (w_z \cos \mu - a) \frac{\partial w_z}{\partial z} + w_u \sin \mu \frac{\partial w_u}{\partial \varphi} + \frac{w_u}{r} \cos \mu \frac{\partial w_z}{\partial \varphi} \right] = \\
& = \rho a^2 c - \rho a (f'_z \cos \mu + f'_u \sin \mu) + \rho a w_r \left( \frac{w_u}{r} + 2\omega \right) \sin \mu + \frac{U M_z}{N_r} \left( a^2 \frac{\partial p}{\partial r} - \frac{\partial p}{\partial r} \right) \quad (45)
\end{aligned}$$

where  $\mu$  represents the angle between the outer normal line and the  $z$  axis at a certain point on the boundary. Equations (42) and (43) are the flow characteristic relations while Equations (44) and (45) correspond to the wave characteristic relations of gas propagating at a speed  $-a$  and  $a$ , respectively.

For the upstream boundary: Let us assume that  $w_{z0} < a$ ; then only Equation (44) can be used. Therefore, three parameters must be given. The other parameters can be obtained from Equation (44). Please notice that because  $\mu = \pi$  at this time, and the three given parameters (e.g.,  $p_0$ ,  $\rho_0$  and gas flow angle) do not vary with time and the parameters along the  $\varphi$  direction are homogeneous, Equation (44) can be drastically simplified.

For the downstream boundary: If the exit gas flow is subsonic at this time, then Equations (42), (43) and (45) are usable relations. It still needs one more given parameter (such as the reverse pressure). Please note that  $\mu = 0$  at this time and, the above three equations can also be simplified. If the exit gas flow is supersonic, then all four relations can be used. We can no longer provide any given parameter.

For the blade surface: Equations (42), (43) and (45) are all applicable. The required boundary condition is that the flow velocity is tangential to the surface.

In addition, there is a periodic condition in the calculation for the  $S_1$  flow surface. Its calculation can be carried out based on the same method as that for the internal points. Of course, when the shock wave extends to the outside of the duct, whether to choose the periodic condition of the suction surface in the pressure surface requires a specific analysis.

## (II) Boundary conditions on the $S_2$ flow surface

The following relations can be obtained at this time:

$$\frac{\partial p}{\partial t} + w_r \frac{\partial p}{\partial r} + w_z \frac{\partial p}{\partial z} - a^2 \left( \frac{\partial p}{\partial t} + w_r \frac{\partial p}{\partial r} + w_z \frac{\partial p}{\partial z} \right) = \frac{\omega N'_k}{N'_k} \left( a^2 \frac{\partial p}{\partial y} - \frac{\partial p}{\partial y} \right) \quad (46)$$

$$\sin \mu' \left( \frac{\partial w_r}{\partial t} + w_r \frac{\partial w_r}{\partial r} + w_z \frac{\partial w_r}{\partial z} + \frac{1}{r} \frac{\partial p}{\partial z} \right) - \cos \mu' \left( \frac{\partial w_z}{\partial t} + w_r \frac{\partial w_z}{\partial r} + w_z \frac{\partial w_z}{\partial z} + \frac{1}{r} \frac{\partial p}{\partial r} \right) =$$

$$= F_z \sin \mu' - \left( F_r + \frac{V_u^2}{r} \right) \cos \mu' \quad (47)$$

$$\frac{\partial p}{\partial t} + (w_r + a \sin \mu') \frac{\partial p}{\partial r} + (w_z + a \cos \mu') \frac{\partial p}{\partial z} + \rho a \left( \cos \mu' \frac{\partial w_r}{\partial t} + \sin \mu' \frac{\partial w_z}{\partial t} \right) +$$

$$+ \rho a \left[ (a + w_r \sin \mu') \frac{\partial w_r}{\partial r} + (a + w_z \cos \mu') \frac{\partial w_z}{\partial z} + w_r \cos \mu' \frac{\partial w_z}{\partial r} + w_z \sin \mu' \frac{\partial w_r}{\partial z} \right] =$$

$$= \rho a^2 \left( c' - \frac{w_r}{r} \right) + \rho a F_z \cos \mu' + \rho a \left( F_r + \frac{V_u^2}{r} \right) \sin \mu' + \frac{\omega N'_k}{N'_k} \left( a^2 \frac{\partial p}{\partial y} - \frac{\partial p}{\partial y} \right) \quad (48)$$

$$\frac{\partial p}{\partial t} + (w_r - a \sin \mu') \frac{\partial p}{\partial r} + (w_z - a \cos \mu') \frac{\partial p}{\partial z} - \rho a \left( \sin \mu' \frac{\partial w_r}{\partial t} + \cos \mu' \frac{\partial w_z}{\partial t} \right) -$$

$$- \rho a \left[ (w_r \sin \mu' - a) \frac{\partial w_r}{\partial r} + (w_z \cos \mu' - a) \frac{\partial w_z}{\partial z} + w_r \cos \mu' \frac{\partial w_z}{\partial r} + w_z \sin \mu' \frac{\partial w_r}{\partial z} \right] =$$

$$= \rho a^2 \left( c' - \frac{w_z}{r} \right) - \rho a F_z \cos \mu' - \rho a \left( F_r + \frac{V_u^2}{r} \right) \sin \mu' + \frac{\omega N'_k}{N'_k} \left( a^2 \frac{\partial p}{\partial y} - \frac{\partial p}{\partial y} \right) \quad (49)$$

where  $\mu'$  represents the angle between the outer normal direction of a point on the boundary and the z-axis. Equations (46) and (47) are the flow characteristic equations, while Equations (48) and (49) are the wave characteristic relations of the corresponding gas propagating at a speed of  $-a$  and  $a$ , respectively.

For the upstream boundary: Let us assume  $W_{z,0} < a$ , then only Equation (48) can be used. Therefore, it needs three given parameters. The other parameter can be obtained from Equation (48). Please note that because  $\mu' = \pi$  and the three given parameters (e.g.,  $P_0$ ,  $\rho_0$  and M number) are time independent and all the parameters in the  $r$  direction are homogeneous, Equation (48) can be greatly simplified.

For the downstream boundary: If the exit flow is subsonic at this time, then Equations (46), (47) and (49) are the applicable relations. It still requires one given parameter (such as the reverse pressure or  $V_u r$ ). Please note that at this time  $\mu' = 0$ , the above three equations can also be greatly simplified. If the exit gas flow is supersonic, then all four relations can all be used. It cannot be provided with any given parameters.

For the up and down walls: Equations (46), (47) and (49) are all applicable. The given boundary condition is that the flow velocity is in the tangential direction to the wall surface.

### (III). Initial conditions

It has already been proven [8] by the theory that the choice of the initial conditions does not affect the final steady solution. However, if the selection of the initial conditions is very improper, it may cause excessive oscillations and damage the stability of the numerical solution. Therefore, the initial values should be chosen so that there is no sudden variation for all the

flow parameters. In the meantime, the selection of the initial values also affect the speed reaching a steady solution. Considering these factors, we can choose the solution of the subsonic flow or the parameter distribution which satisfies the continuity equation on the geometric center line and appears to be smooth elsewhere as the initial condition.

#### VI. THE PROCEDURES OF OBTAINING THE COMPLETE SOLUTION OF THREE-DIMENSIONAL FLOW

We have already transformed the problem of the three-dimensional flow with shock waves in turbine machinery into two families of initial value-boundary value problems of hyperbolic equations with three variables. It also presents the methods to determine the initial and boundary conditions and then completely establishes the specific solution problems for the two types of unsteady four-dimensional flow surfaces. In order to obtain the solution of the three-dimensional flow, besides the steady solutions of the initial value-boundary values problems on the two families of flow surfaces, we must carry out iteration between each other until it becomes convergent.

In order to save the calculation time, we can use the time progressing and flow surface iteration method. For the calculation of each step of  $\Delta t_j$  or several steps of  $\Sigma \Delta t_j$ , we carry out an iteration between the two families of flow surfaces. This involves giving the results of each flow surface calculation and the shape of each four-dimensional flow surface (see Equation (1)) to the other flow surface to carry out the calculation for the next time interval. It repeats itself regardless of whether a steady solution is reached in each calculation. When the steady solution is nearly obtained, iteration between flow surfaces is required for every time interval. Of course, it is not required to have a completely steady solution. Finally, when steady solutions are obtained on

all the flow surfaces, the final solution of the entire three-dimensional flow is obtained.

Such procedures to obtain the solution clearly demonstrate what has been pointed out in [2] that this method cannot be used to solve a transonic flow with shock wave on a given flow surface. In other words, it is through the continuous adjustment of the position and shape of the flow surface during the solution seeking process which makes it possible to obtain the two dimensional shock waves which are consistent with the spatial shock wave on the two families of flow surfaces. The above procedures closely combine the calculated shock wave on a single flow surface with the spatial shock wave so that the time needed to obtain a steady solution can be reduced.

## VII CONCLUSIONS

On the basis of extending the three-dimensional flow surface model to the four-dimensional unsteady flow surfaces, this paper transformed the ordinary equations of the non-viscous adiabatic gas flow in turbine machinery to two types of unsteady flow surfaces  $S_1$  and  $S_2$  and then re-established the corresponding basic equations. Comparing these equations with those for corresponding steady flow surfaces, we found that, in addition to the presence of the partial derivatives of the thickness of the flow sheet vs. time, the shape of the four-dimensional flow surface has a certain contribution toward  $c$  (or  $c'$ ) and the "flow sheet force". In the energy equation, there is also a related term  $\epsilon$  (or  $\epsilon'$ ). These equations are applicable to the unsteady flow or the steady flow with shock waves.

It should be pointed out that the equations used to obtain solutions to the transonic flow problem in the literature to date on the flow surfaces (mainly revolving surfaces) are for time independent flow surfaces. The thickness of the flow sheet is also not

related to time. Therefore, the shock wave thus calculated is not a part of the real shock wave in the space. Actually, the basic equations used in the literature are not obtained from the basic equations used to solve for the spatial shock waves. They are merely equations with the arbitrary addition of unsteady terms to the steady flow equations. The result is that it failed to consider the close relations between the two families of flow surfaces under the conditions that shock wave existed.

Based on the characteristic curve theory, we derived the characteristic relations between the two types of surfaces and further determined the boundary conditions for the condition of steady flow with shock waves. There is a certain degree of flexibility in the selection of the initial conditions. The proper choice of the initial condition can completely define the specific solution problem of transonic flow with shock wave on the two types of flow surfaces.

Considering the close relation between the flow surfaces when there are shock waves, in order to obtain the solution of the three-dimensional flow, we can use the time progressing and flow surface iterations method to save the calculation time. Thus, after the difference format is chosen, we can obtain the solution numerically.

#### REFERENCES

- [1] Wu C. H. (吳仲華). A general theory of three-dimensional flow in subsonic and supersonic turbo-machines of axial, radial, and mixed-flow types, NACA TN 2604, 1952.
- [2] Hsu Tsen-chung. "Relation of Shock Waves in Turbomachines", Technical Report of the Institute of Mechanics, Academy of Science, China, Aug. 1978.

- [3] Courant R. and Hilbert D.: *Methods of mathematical physics*, vol. II, 1962.
- [4] Giang A. and Serra R.: *Boundary conditions and Uniqueness in Internal Gas Dynamic Flows*, AIAA J., vol. 12, No. 3, Mar. 1974, p. 263.
- [5] Gopalakrishnan S. and Bezzola R.: *Numerical representation of inlet and exit boundary conditions in transient cascade flow*, ASME paper 73-GT-55.
- [6] Богод А. Б., Замфорт Б. С., Ивнов М. Я. и Крайко А. Н.: Об использовании процесса установления по времени при решении задач стационарного обтекания газом решток профилей, *Механика Жидкости и Газы*, № 4, 1974, стр. 118.
- [7] Veilliot J.-P.: *Calcul numérique de l'écoulement transsonique d'un fluide parfait dans une grille d'aubes*, La Recherche Aérospatiale, No. 6, 1975, p. 327.
- [8] Lax P.: *Weak solutions of nonlinear hyperbolic equations and their numerical computation*, *Comm. Pure Appl. Mech.*, vol. 7, 1954, p. 159.

LMED  
-8